NUREG/CR-4651
ORNL/TM-10100

Development of Riprap Design Criteria by Riprap Testing in Flumes: Phase I

Prepared by S. R. Abt, M. S. Khattak, J. D. Nelson,
J. F. Ruff, A. Shaikh, R. J. Wittler/CSU
D. W. Lee, N. E. Hinkle/ORNL

Colorado State University

Oak Ridge National Laboratory

**Prepared for
U.S. Nuclear Regulatory
Commission**

NUREG/CR-4651
ORNL/TM-10100

Development of Riprap Design Criteria by Riprap Testing in Flumes: Phase I

Manuscript Completed: October 1986
Date Published: May 1987

Prepared by
S. R. Abt, M. S. Khattak, J. D. Nelson, J. F. Ruff,
A. Shaikh, R. J. Wittler, Colorado State University
D. W. Lee, N. E. Hinkle, Oak Ridge National Laboratory

Colorado State University
Fort Collins, CO 80523

Under Contract to:
Oak Ridge National Laboratory
Oak Ridge, TN 37831

Prepared for
Uranium Recovery Field Office
Region IV - Box 25325
U.S. Nuclear Regulatory Commission
Denver, CO 80401
and
Division of Waste Management
Office of Nuclear Material Safety and Safeguards
U.S. Nuclear Regulatory Commission
Washington, DC 20555
NRC FIN A9350

ABSTRACT

Flume studies were conducted in which riprap embankments were subjected to overtopping flows. Embankment slopes of 1, 2, 8, 10 and 20% were protected with riprap layers with median stone sizes of 1, 2, 4, 5 and/or 6 inches. Riprap design criteria for overtopping flows were developed in terms of unit discharge at failure, interstitial velocities and discharges through the riprap layer, resistance to flow over the riprap surface, potential impacts of the filter blanket on the riprap layer stability, and the effects of flow concentrations on the riprap stability. The resulting riprap design criteria were compared to the Stephenson, the U.S. Army Corps of Engineers, the U.S. Bureau of Reclamation, and the Safety Factors methods for riprap stone design; the Leps relation for interstitial velocities through riprap; and the Anderson et al. and Corps of Engineers relationships for estimating Manning's n values for resistance to flow.

TABLE OF CONTENTS

LIST OF FIGURES

LIST OF TABLES

NOTATION

Symbol	Term
A	Cross-sectional area of flow
a	coefficient
C	Constant
C_c	Bed critical Shield's coefficient
C_f	Concentration factor
CSU	Colorado State University
COE	U.S. Army Corps of Engineers
C_u	Coefficient of uniformity
C_z	Coefficient of gradation
D	Depth of flow
D_x	Soil diameter at which x percent of the soil weight is finer
D_{50}	Median stone size
e	Void ratio
F	Froude number
F_d	Drag force
F_l	Lift force
f	Darcy-Weisbach friction factor
G_s	Specific gravity
g	Acceleration of gravity
i	Slope of embankment
K	Oliviers' constant
k	Equvalent channel boundary surface roughness
n	Manning's roughness coefficient

Symbol	Term
n_{CSU}	Manning's roughness coefficient determined from tests performed at CSU
n_{COE}	Manning's roughness coefficient determined from U.S. Army Corps of Engineers methods
n_{ANDER}	Manning's roughness coefficient determined from Andersons's method
n_p	Porosity
Q	Channel discharge
Q_c	Total channel discharge
Q_f	Failure discharge
Q_I	Interstitial discharge
Q_S	Surface discharge
Q_T	Total discharge
q	Unit discharge
q_c	Unit flow rate through channel
q_f	Unit failure discharge
q^*_m	Stephenson's unit threshold flow at which movement of stones commences
q_f^{**}	Stephenson's unit failure flow rate
q^*	Unit discharge per inch of riprap thickness
R	Hydraulic radius of channel
R_e	Reynolds number
r^2	Regression coefficient
S	Slope of embankment
S_m	Safety factor of riprap rolling down with no flow
SF	Safety Factors method

Symbol	Term
STEPH	Stephenson's method
t	Time elapsed after starting the test
t_f	Total time of test
USBR	U.S. Bureau of Reclamation
V	Surface flow velocity
V_b	Localized bottom velocity of flow
V_{max}	Maximum localized surface velocity
V_{CSU}	Interstitial velocity determined from tests performed at CSU
V_{Leps}	Interstitial velocity determined from Leps method
W_m	Emperical constant
W_s	Weight of stone
α	Slope angle
β	Wave front angle
γ	Unit weight
γ_s	Unit weight of surface-dry but saturated stone
γ_w	Unit weight of water
η	Stability number for riprap on a plane bed
η'	Stability number for riprap on a side slope
θ	Angle of slope measured from horizontal
ϕ	Friction angle
λ	Angle between horizontal and velocity vector
ν	Kinematic viscosity
τ	Shear stress
τ_0	Bed shear stress
$\bar{\tau}_0$	Local boundary shear stress

ACKNOWLEDGMENTS

Research performed by Colorado State University under Subcontract No. ORNL-19X-077326 from Oak Ridge National Laboratory, operated by Martin Marietta Energy Systems, Inc. under Contract No. DE-AC05-840R21400 with the U.S. Department of Energy. Research sponsored by Office of Nuclear Material Safety and Safeguards, U.S. Nuclear Regulatory Commission.

The authors express their appreciation to the Colorado State University staff involved in the construction, testing and data reduction phases of this project. Individuals acknowledged for their participation include Mr. Khaled Mahmoud Abu-Zeid, Mr. Fred Doehring, Mr. Pablo Gomez, Mr. Scott Hawley, Mr. David LaGrone, Mr. Louis Miller, Mr. Michael Ruff, Mr. Roger Schlomann, and Mr. Karsten Thompson.

1. INTRODUCTION

1.1 GENERAL

The protection of the public health and environment from the potential hazards of waste materials has stimulated the assessment of waste stabilization design procedures and methods. Current stabilization methods cap the waste materials with an earthen cover. Reclamation standards require that waste impoundments be designed and constructed to insure the long-term stabilization for periods of 200 to 1000 years.

One means of providing long-term stabilization of a waste impoundment is to place a protective filter blanket and riprap layer over the cover. Nelson et al. (1986) indicated that when riprap protection is considered, alternative design procedures should be used for different zones of the impoundment. The riprap design should protect the impoundment from regional and localized flooding conditions which affect the embankment toe and side slopes in the flood plain.

Furthermore, riprap design procedures should also protect the impoundment cap and side slopes from overtopping flows that may occur. The riprap design procedures must be conservative enough to insure cover stabilization yet be economically advantageous to warrant the use of riprap. Established and field tested design procedures exist that stabilize embankment toes and bank slopes for traditional channel flow conditions. Unfortunately, an established, field tested design procedure for application in overtopping situations is not available.

1.2 OBJECTIVES

The objective of this investigation was to provide riprap design criteria for overtopping flows. A series of laboratory experiments were conducted to:

(a) Determine the unit discharge, slope, and stone size relationships of a riprap system at incipient failure;

(b) Determine the interstitial velocities within the riprap layer;

(c) Determine the resistance to surface flows over the riprap; and,

(d) Identify the effects of the filter blanket, flow channelization, and time on the riprap stability.

The results of the experimental program are compared to existing design procedures where applicable.

2. DESCRIPTION OF FACILITIES AND ARMORING MATERIALS

2.1 INTRODUCTION

The experimental program was conducted in two flume facilities located at the Engineering Research Center of Colorado State University. An outdoor flume was utilized for simulating steep, embankment side slopes ($\geq$ 10%) while an indoor laboratory flume was used for simulating flat slopes (< 10%). Each flume was modified to enable prototype testing of riprap covered slopes to evaluate the flow conditions and the stability of the riprap layer.

2.2 OUTDOOR FACILTY

The outdoor facility (flume 1a) is a concrete flume that is 180-feet (54.9 m) long, 20-feet (6.1 m) wide, and 8-feet (2.4 m) deep. The flume is shown in Fig. 2.1. The flume was modified so that the upper 20 feet served as an inlet basin for energy dissipation and wave suppression. A head wall was constructed and served as the inlet to the test section. The throat of the test section was twelve feet wide to allow a concentration of flow onto the embankment. The test embankment extended 40 feet downstream of the headwall. The remainder of the flume was used for tailwater control and material recovery.

Water was supplied to the facility from Horsetooth Reservoir through an existing pipe network. A 36-inch butterfly valve located just upstream of

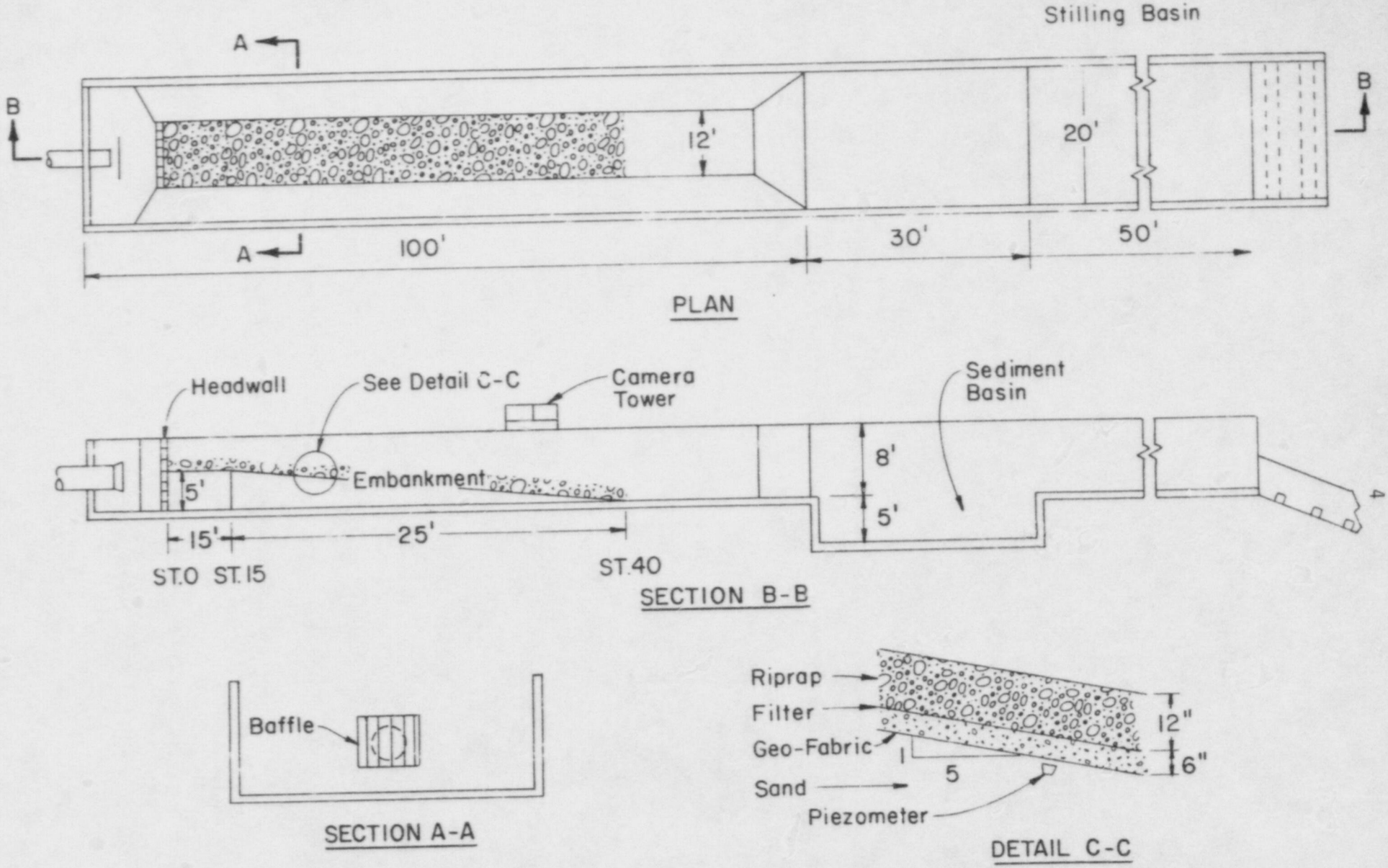

Fig. 2.1. Outdoor flume (1a) schematic.

the flume served to control inflow to the inlet basin. A sonic flow meter was used to determine inlet discharges.

The test embankment was constructed of a moistened, compacted sand in the test section. The initial 15 feet of the embankment was horizontally placed simulating the top of a tailings pile. The embankment transitioned to a 20% slope simulating the steep side slope of a reclaimed tailings pile. Geofabric was used to cover and stabilize the sand embankment. The geofabric allowed the embankment to be saturated and to move under a variety of loading conditions. However, the geofabric prevented the sand embankment from massive failure thereby minimizing turn-around time between experiments.

A 6-inch thick sand/gravel filter layer was placed on top of the geofabric as specified by the appropriate filter design criteria for most of the tests. Riprap was placed on top of the filter material to the prescribed layer thickness.

A catwalk and observation platform were constructed and placed on top of the flume. The catwalk served to allow access to any portion of the test section for data acquisition. The observation platform was used for video taping each record test.

2.3 INDOOR FACILITY

The indoor facility (flume 1b), located in the Hydraulic Laboratory, is a steel flume that is 200-feet (61 m) long, 8-feet (2.4 m) wide, and 4-feet (1.2 m) deep as shown in Fig. 2.2. The flume is mounted on top of jacks

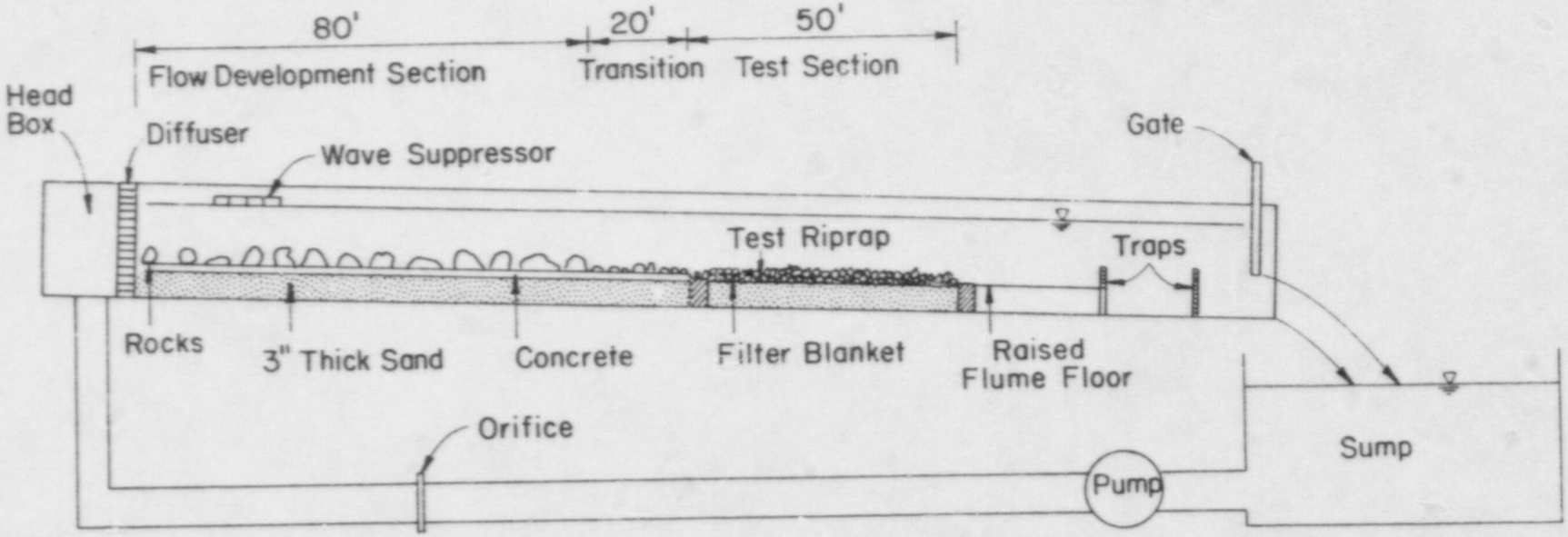

Fig. 2.2. Indoor flume (1b) schematic.

that allow the slope to vary from 0 to 3%. The pumping system is capable of circulating up to 100 cfs. Discharges were measured with orifices located in the water supply pipelines

The flume inlet was modified so flows entered the head box, discharged through a diffuser, and transitioned into the flow development section. Rock was fixed in the upstream 80 feet of the flume to establish uniform turbulent approach flow conditions in the channel. A 20-foot transition section was constructed linking the approach to the 50-foot riprap test section. The remainder of the flume served as the tailwater control and material recovery basin. The test embankment consisted of a moistened, compacted 4-inch sand layer. Geofabric was used to cover and stabilize the sand bed. An appropriately sized sand/gravel filter was placed on the geofabric to a thickness of approximately 6 inches. Riprap was placed on top of the filter material to the prescribed layer thickness.

The embankment was constructed to simulate the top of a tailings pile. Therefore, the majority of the tests were conducted at slopes of 2% or less. However, the test section was modified to accommodate 8% and 10% slopes. The modified slopes were constructed similar to slopes in the outdoor facility.

A motorized carriage spanned the flume and was used to support data acquisition and videotaping equipment. The carriage allowed access to any location in the flume.

2.4 INSTRUMENTATION

The instrumentation consists of the equipment to monitor the water surface elevation and flow velocity through and over the riprap layer. Portable television equipment was utilized to videotape and photograph the riprapped embankments prior to, during, and after testing.

A tracer solution injection and recording system was developed to document the flow velocities through the riprap layer. The system was composed of a pressure-operated tracer injector, tracer-sensitive probes, multi-channel selector, and multi-channel strip chart recorder as shown in Fig. 2.3. Each tracer-sensitive probe was fabricated with three tracer-sensitive elements placed in the lower 8 inches of the probe. Salt was used as the tracer.

The tracer-sensitive system was placed in the riprap layer such that the injector ports were approximately aligned with the tracer-sensitive elements. The injector and probes were 10-12 inches and 20-24 inches apart. The flow was established such that the water surface was at an elevation halfway through the riprap layer, at the top of the riprap layer, and just above the riprap surface in sequential tests. An event marker on a strip chart recorder indicated when the injector was triggered. Output from the tracer-sensitive elements were also recorded on the strip chart enabling the tracer dilution curve to be observed. Flow velocities were derived from the tracer-dilution curves recorded on the strip chart for each flow condition and riprap layer thickness.

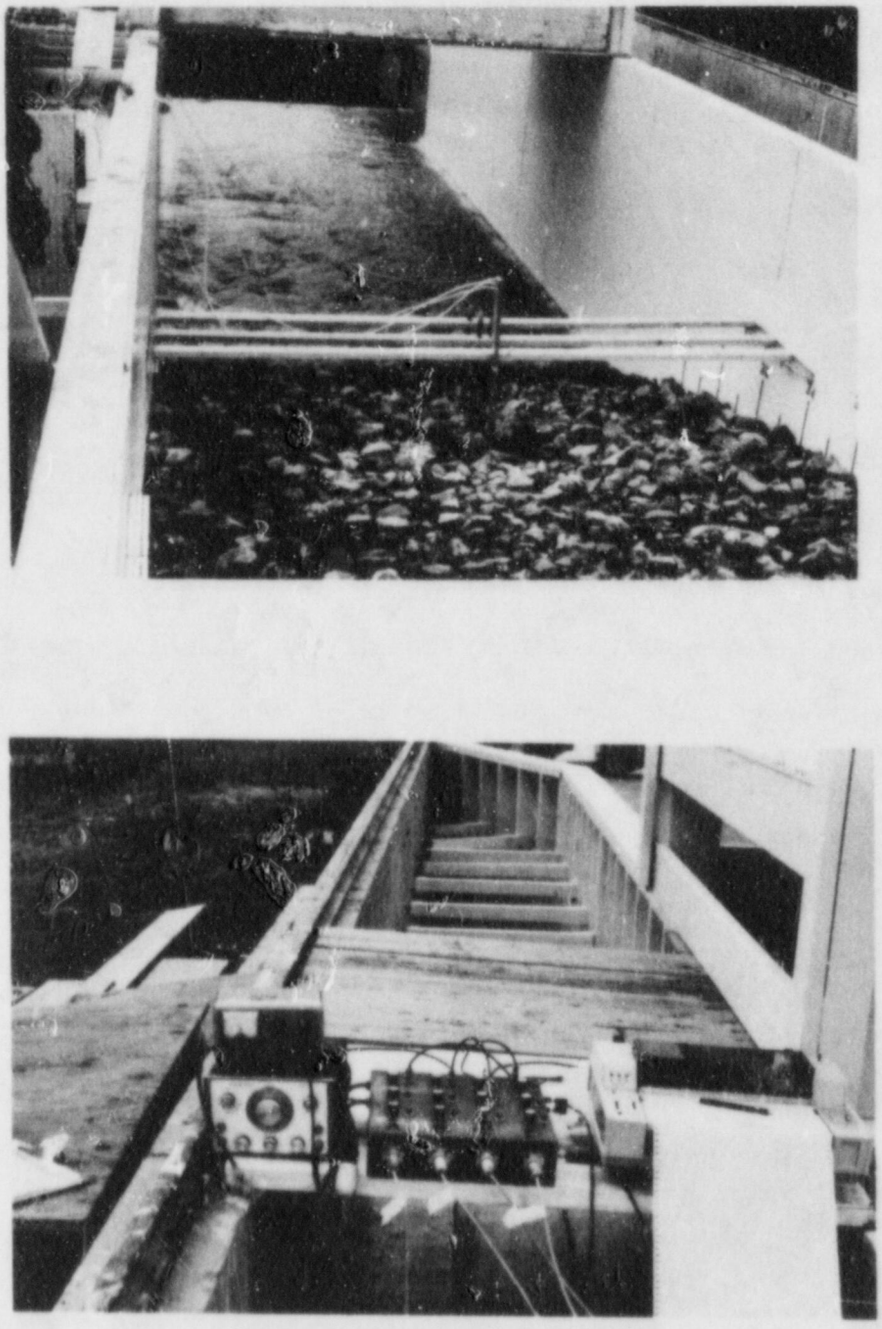

Fig. 2.3. Tracer injection and recording system.

Surface velocities in the outdoor flume were measured using a Marsh-McBirney® magnetic flow meter. The meter was periodically calibrated throughout the experimental program. A pitot tube was used to determine the velocity profiles in the indoor flume.

Water surface elevations were monitored using piezometers installed in the embankments of both flumes. Piezometers were placed at sections near the crest of the embankment, at the mid-point of the slope, and at the toe of the slope of each embankment. The piezometers were equally spaced across each section to monitor potential differences in the flow distribution. Each piezometer was connected to a manometer board to enable the recording of the water surface elevation.

A Panasonic videotape camera and VCR recording system were used to visually document each failure test. Also, photographic equipment documented pre-test, test, and post-test embankment conditions.

2.5 RIPRAP PROPERTIES

The riprap was obtained from a quarry located near Denver, Colorado. Nominal median stone sizes (D_{50}) tested were 1, 2, 4, 5 and 6 inches. Rock properties of gradation, unit weight, specific gravity, porosity, void ratio and friction angle were determined in the Colorado State University Geotechnical Engineering Laboratory using procedures outlined by the American Society for Testing Materials (ASTM). A summary of the riprap properties are presented in Table 2.1. The grain size distribution for each riprap and the associated filter material are presented in Appendix 1.

Table 2.1. Riprap properties.[a]

D_{50} (in.) Nominal	D_{50} (in.) Actual	C_u	C_z	γ (lb/ft^3)	G_s	n_p	e	ϕ	Shape
1.0	1.02	1.75	1.28	94	2.72	0.44	0.79	40	Sub-Angular
2.0	2.2	2.09	1.26	92	2.72	0.45	0.84	41	Angular
4.0	4.1	2.15	1.12	92	2.65	0.44	0.78	42	Angular
5.0	5.1	1.62	1.02	90	2.65	0.46	0.85	42	Angular
6.0	6.2	1.69	1.08	90	2.65	0.46	0.85	42	Angular

[a] All properties were determined in the Colorado State University Geotechnical Laboratory in accordance with ASTM guidelines with the following definitions.

D_{50} = median stone size

C_u = Coefficient of uniformity $\left[C_u = \frac{D_{60}}{D_{10}}\right]$

C_z = Coefficient of graduation $\left[C_z = \frac{D_{30}^2}{(D_{10})(D_{60})}\right]$

γ = Unit weight

G_s = Specific gravity

n_p = Porosity

e = Void ratio

ϕ = Friction angle

A filter blanket underlaid the riprap layer in most of the tests. The filter criteria used to size the blanket was derived from Sherad et al. (1963) and is expressed as

$$\frac{D_{15}(\text{riprap})}{D_{85}(\text{filter})} < 5 \tag{2.1}$$

$$5 < \frac{D_{15}(\text{riprap})}{D_{15}(\text{filter})} < 40 \tag{2.2}$$

$$\frac{D_{50}(\text{riprap})}{D_{50}(\text{filter})} < 50 \tag{2.3}$$

3. EXPERIMENTAL PROGRAM

3.1 TEST VARIABLES

A series of 52 experiments were conducted including shakedown, rock movement, interstitial flow, and rock failure. A summary of the experimental program is presented in Table 3.1. The experimental variables encompassed the median stone size, D_{50}, embankment slope, S, presence of a filter blanket, and the discharge rate, Q. The data collected during each experiment included the surface and/or interstitial flow velocities, V, water surface elevations, and time. Test results for the two flumes were reduced by converting the discharge rate, Q, to unit discharge, q, which is the discharge per unit width.

General observations were recorded, when appropriate, to document flow and riprap phenomena which could not be physically measured. For example, incipient flow concentrations, filter blanket extraction and failure, riprap layer failure indicators, and stone movement (beyond bed adjustment) could not explicitly be measured. Therefore, qualitative observations during each test, and later verified during videotape playback, were recorded and incorporated into the analysis.

Riprap was dump-placed in all the tests conducted in this phase of the study. However, the stone surface was leveled to minimize the occurrence of man-made flow concentrations. The riprap layer thickness was determined using a self-leveling level. Predetermined locations on the filter served as a reference. Once the rock layer was graded, a square plate was placed

Table 3.1. Summary of experimental program.

No. Tests	Riprap Size Nominal D_{50} (inches)					Slope %					Filter Blanket	Flume
	1	2	4	5	6	1	2	8	10	20		
6	x					x					x	8'
11	x						x				x	8'
4	x								x		x	8'
7		x					x				x	8'
1		x						x			x	8'
3		x							x		x	8'
3		x								x		12'
3		x								x	x	12'
5			x							x	x	12'
4				x						x	x	12'
5					x					x	x	12'
52												

on top of the rock and the elevation was calculated. The difference between the top of the filter blanket and top of the rock layer was the layer thickness.

3.2 TEST PROCEDURE

The rock movement and riprap failure test procedures were similar for all 52 experiments conducted in both indoor and outdoor facilities. Once the test embankment and riprap were placed and the instrumentation set and checked, the flume inlet valve was opened. The riprap was inundated and the bed was allowed to adjust and/or settle. The flow was increased until surface flow was observed. Once the flow stabilized, the discharge was determined and localized velocities and water surface elevations were obtained along four cross sections when and where possible. After recording the data and documenting observations, the flow was increased. Generally, 12-20 minutes were required to increase and stabilize the flow, acquire data, and record results. The procedure was repeated until stone movement and/or failure occurred. In several instances the stone movement tests were extended to failure. A videotape recording was made of portions of each test.

3.3 PARAMETERS OF ANALYSIS

The Manning's roughness coefficient, n, bed critical Shields' coefficient, C_c, and Darcy-Weisbach friction factor, f, were computed for each discharge tested.

3.3.1 Manning's Roughness Coefficient

The Manning's roughness coefficient (Chow, 1959) can be estimated as

$$n = \frac{1.486}{Q} A R^{2/3} S^{1/2} \qquad (3.1)$$

where

n = Manning's roughness coefficient for the bed

S = Channel slope (ft/ft)

A = Cross-sectional area of flow (ft^2)

Q = Channel discharge (cfs) of surface flow

R = Hydraulic radius of channel (ft)

The ratio of depth of flow to transverse width of the embankment was on the order of 0.05 or less and considered relatively small. Therefore, the channel was assumed to be a wide channel. Since the depth of flow, D, is approximately equal to the hydraulic radius for a wide channel, Eq. 3.1 can be modified to

$$n = \frac{1.486}{Q} A D^{2/3} S^{1/2} \qquad (3.2)$$

3.3.2 Shields' Coefficient

The bed critical Shields' coefficient (Simons and Senturk, 1977) is an indicator of incipient stone movement on the rock bed. The Shields' coefficient (C_C) is defined as

$$C_C = \frac{DS}{(G_S-1)\ D_{50}} \qquad (3.3)$$

where

D = Depth of flow (ft)

S = Channel slope (ft/ft)

G_S = Specified gravity of the rock

D_{50} = Median stone size of the riprap (ft)

3.3.3 Darcy-Weisbach Friction Factors

The Darcy-Weisbach friction factor (Ruff et al., 1985) was computed for each test discharge. The Darcy-Weisbach friction factor (f) is defined as

$$f = \frac{8\ g\ D\ S}{V^2} \qquad (3.4)$$

where

g = Acceleration of gravity (ft/s^2)

V = Average velocity of flow (ft/s)

D = Depth of flow (ft)

S = Channel slope (ft/ft)

3.4 ESTABLISHED DESIGN PROCEDURES

Presently, several riprap design procedures are routinely used to determine the appropriate stone size for protection of impoundment covers,

embankments, channel and unprotected slopes from the impact of flowing waters. Four riprap design procedures which will be referenced are:

1. Safety Factors Method (SF)
2. The Stephenson Method (STEPH)
3. The U.S. Army Corps of Engineers Method (COE)
4. The U.S. Bureau of Reclamation Method (USBR)

A summary of each method will be presented.

3.4.1 Safety Factors Method

The Safety Factors Method (Richardson et al., 1975) for sizing riprap allows the designer to evaluate rock stability from flow parallel to the cover and adjacent to the cover. The Safety Factors Method can be used by assuming a stone size and then calculating the safety factor (SF) or allowing the designer to determine a SF and then computing the corresponding stone size. If the SF is greater than unity, the riprap is considered safe from failure; if the SF is unity, the rock is at the condition of incipient motion; and if SF is less than unity, the riprap will fail.

The following equations are provided for riprap placed on a side slope or embankment where the flow has a non-horizontal (downslope) velocity vector. The safety factor, SF, is:

$$SF = \frac{\cos \theta \tan \phi}{\eta' \tan \phi + \sin \theta \cos \beta} \tag{3.5}$$

where

$$\eta' = \eta \left[\frac{[1 + \sin (\lambda + \beta)]}{2} \right] \tag{3.6}$$

$$\eta = \frac{21 \tau_o}{(G_s - 1) \gamma D_{50}} \tag{3.7}$$

$$\tau_o = \gamma DS \tag{3.8}$$

and

$$\beta = \tan^{-1} \left[\frac{\cos \lambda}{(2 \sin\theta)/(\eta \tan\phi) + \sin \lambda} \right] \tag{3.9}$$

The angle, λ, is shown in Figure 3.1 and is the angle between a horizontal line and the velocity vector component measured in the plane of the side slope. The angle, θ, is the side slope angle shown in Figure 3.1 and β is the angle between the vector component of the weight, W_s, directed down the side slope and the direction of particle movement. The angle, ϕ, is the angle of repose of the riprap, τ_o is the bed shear stress (Simons and Senturk, 1977), D_{50} is the representative stone size, G_s is the specific gravity of the rock, D is the depth of flow, γ is the specific weight of the liquid, S is the slope of the channel, and η' and η are stability numbers. In Figure 3.1, the forces F_l and F_d are the lift and drag forces, and the moment arms of the various forces are indicated by the value e_i as i = 1 through 4. Figure 3.2 illustrates the angle of repose for riprap material sizes.

Riprap is often placed along side slopes where the flow direction is close to horizontal or the angularity of the velocity component with the

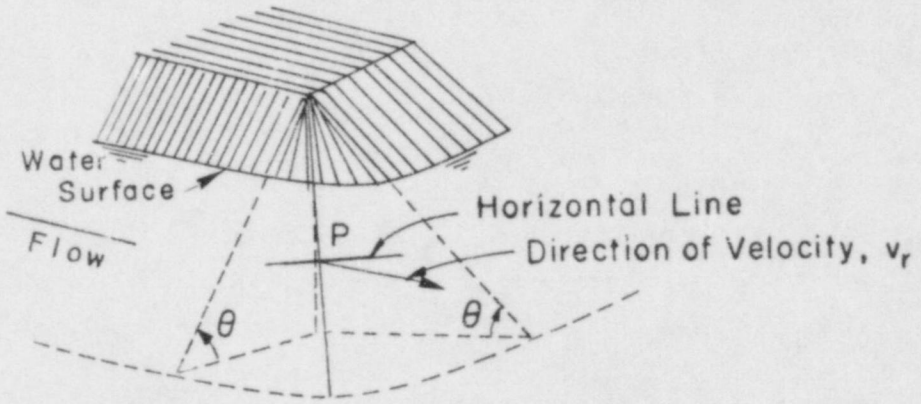

(a) General View

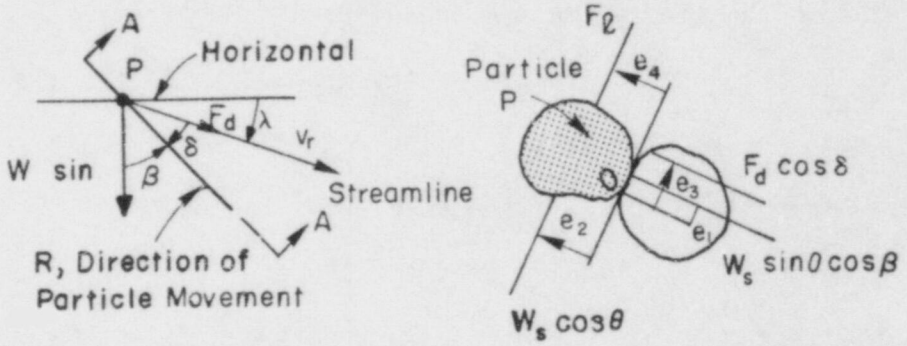

(b) View Normal to the Side Slope (c) Section A-A

Fig. 3.1. Riprap stability conditions as described in the Safety Factors Method.

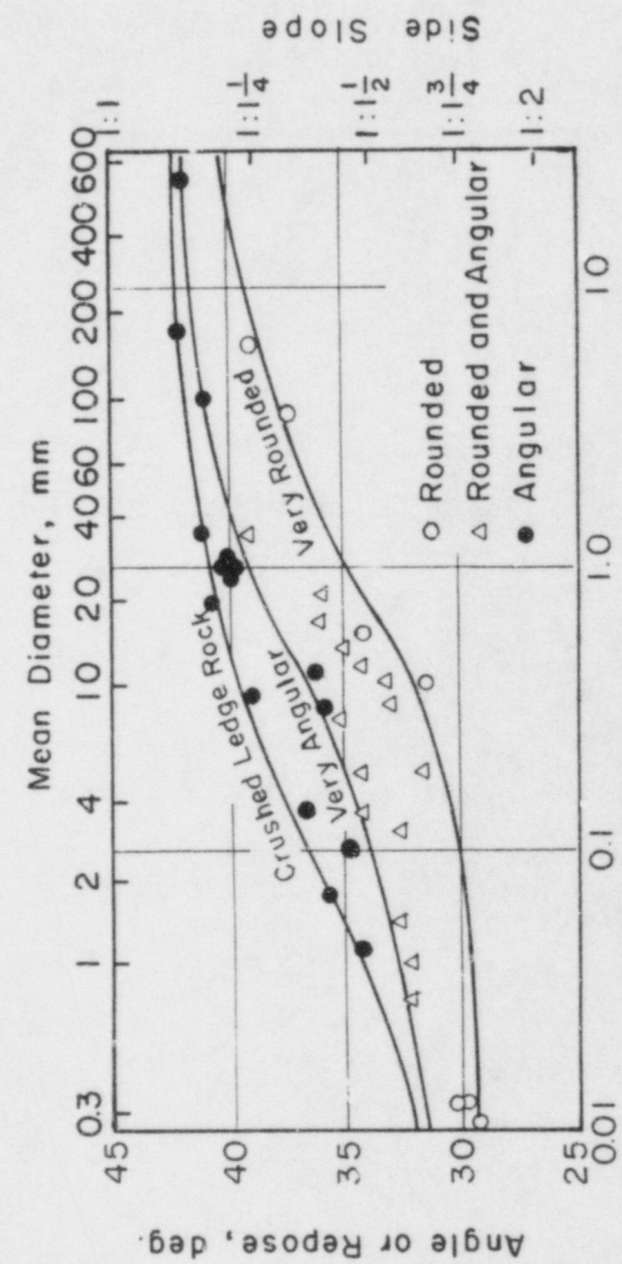

Fig. 3.2. Angle of repose as a function of median stone diameter and shape.

horizontal is small (i.e., $\lambda = 0$). For this case, the above equations reduce to:

$$\tan \beta = \frac{n \tan \phi}{2 \sin \theta} \tag{3.10}$$

and

$$\eta = \left[\frac{S_m^2 - (SF)^2}{(SF)\ (S_m^2)} \right] \cos \theta \tag{3.11}$$

where

$$S_m = \frac{\tan \phi}{\tan \theta} \tag{3.12}$$

The term S_m is the safety factor of the rock particles against rolling down the slope with no flow. The safety factor, SF, for horizontal flow may be expressed as:

$$SF = \frac{S_m}{2} [S_m^2 \eta^2 \sec^2 \theta + 4)^{0.5} - S_m \eta \sec \theta] \tag{3.13}$$

Riprap may also be placed on the cover or side slope. For a cover sloping in the downstream direction at an angle, α, with the horizontal, the equations reduce to:

$$SF = \frac{\cos \alpha \tan \phi}{\eta \tan \Phi \sin \alpha} \tag{3.14}$$

Historic use of the Safety Factors Method has indicated that a minimum SF of 1.5 for non-PMF applications (i.e. 100-year events) provides a side slope with reliable stability and protection (Simons and Senturk, 1977). However, a SF of slightly greater than 1.0 is recommended for PMF or maximum credible flood circumstances. It is recommended that the riprap thickness be a minimum of 1.5 times the D_{50}. Also, a bedding or filter layer should underlay the rock riprap. The filter layer should minimally range from 6 inches to 12 inches in thickness. In cases where the Safety Factors Method is used to design riprap along embankments or slopes steeper than 4H:1V, it is recommended that the toe be firmly stabilized.

3.4.2 Stephenson Method

The Stephenson Method for sizing rockfill to stabilize slopes and embankments is an empirically derived procedure developed for emerging flows (Stephenson, 1979). The procedure is applicable to a relatively even layer of rockfill acting as a resistance to through and surface flow. It is ideally suited for the design and/or evaluation of embankment gradients and rockfill protection for flows parallel to the embankments, cover or slope.

The sizing of the stable stone or rock requires the designer to determine the maximum flow rate per unit width (q), the rockfill porosity (n_p), the acceleration of gravity (g), the relative density of the rock (G_s), the angle of the slope measured from the horizontal (θ), the angle of friction (ϕ), and the empirical factor (C).

The stone or rock size, D_{50}, is expressed by Stephenson as

$$D_{50} = \left[\frac{q(\tan\theta)^{7/6} n_p^{1/6}}{C\, g^{1/2} [1-n_p)(G_s-1) \cos\theta\, (\tan\phi - \tan\theta)]^{5/3}} \right]^{2/3} \qquad (3.15)$$

where the factor C varies from 0.22 for gravel and pebbles to 0.27 for crushed granite. The stone size calculated in Equation 3.15 is the representative diameter, D_{50}, at which rock movement is expected for unit discharge, q. The representative median stone diameter (D_{50}), is then multiplied by Oliviers' constant, K, to insure stability. Oliviers' constants are 1.2 for gravel and 1.8 for crushed rock. The rockfill layer should be well graded and at least two times the D_{50} in thickness. A bedding layer or filter should be placed under the rockfill.

The Stephenson Method does not account for uplift of the stones due to emerging flow. This procedure was developed for flow over and through rockfill on steep slopes. Therefore, it is recommended that the Stephenson Method be applied as an embankment stabilization for overflow or sheetflow conditions. Alternative riprap rockfill design procedures should be considered for toe and stream bank stabilization.

3.4.3 U.S. Army Corps of Engineers Method

The U.S Army Corps of Engineers has developed perhaps the most comprehensive methods and procedures for sizing riprap revetment. Their criteria are based on extensive field experience and practice (COE, 1970 and

1971). The U.S. Army Corps of Engineers Method is primarily applicable to embankment toe and bank protection and has been developed to protect the embankment from local shear forces and localized velocities.

The toe of a slope or embankment is generally subjected to the greatest concentration of erosive forces and therefore must be protected. The effective stone size, D_{50}, can be estimated after the depth of flow, D, is determined. The local boundary shear, $\bar{\tau}_0$ can be computed as

$$\bar{\tau}_0 = \frac{\gamma_w V^2}{(32.6 \log_{10} \frac{12.2 D}{k})^2} \tag{3.16}$$

where γ_w is the unit weight of water in pounds per cubic foot, V is the average cross-sectional velocity in ft/s, k is the equivalent channel boundary surface roughness in feet, and D is the depth of flow in ft. By substituting D_{50} for k, the local boundary shear at any point on the wetted perimeter can be determined. The design shear stress, τ_0, should be based on critical local velocities and shall serve as the design shear for the toe and channel bottom. A graphic solution to Equation 3.16 is presented in Figure 3.3.

The design shear for riprap placed on the channel slope or bank can be determined as

$$\tau_0 = \tau \left[1 - \frac{\sin^2 \theta}{\sin^2 \phi} \right] 0.5 \tag{3.17}$$

as

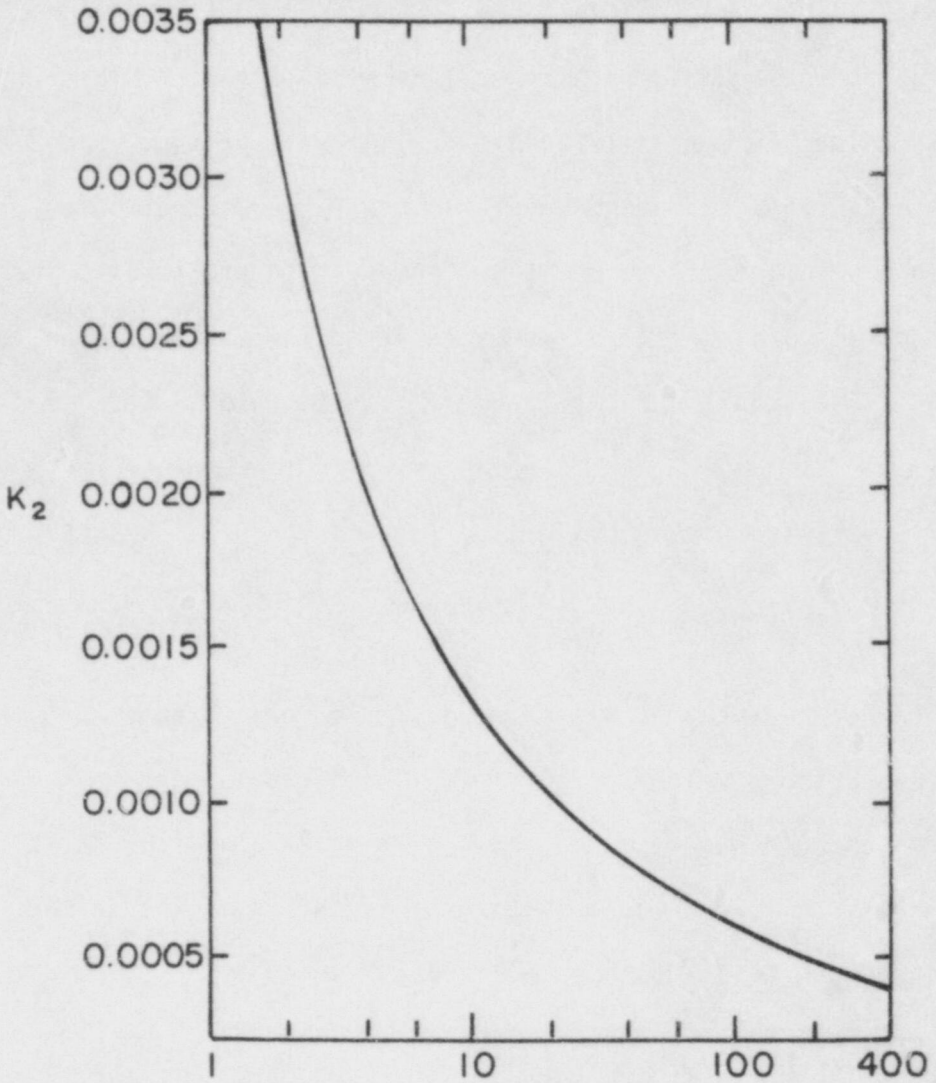

Basic Equation

$$\tau_0 = K_2 V^2$$

where

$$K_2 = \frac{\gamma_w}{\left[32.6 \log_{10}(12.2\, D/D_{50})\right]^2}$$

γ_w = Specific Weight of Water

D = Flow Depth

D_{50} = Theoretical Spherical Diameter of Average Stone Size

Fig. 3.3. Graphical solution to Eq. 3.16. Source: COE, 1970.

$$\tau = a(\gamma_s - \gamma_w) D_{50} \tag{3.18}$$

where θ is the angle of the side slope with the horizontal, ϕ is the angle of repose of the riprap (normally about 40°), γ_s is the unit weight of surface dry but saturated stone, and the value of a is 0.04. The side slope shear, τ_o, is the design shear for sizing the riprap revetment.

The average stone size can then be determined as

$$D_{50} = \frac{\tau}{0.04\ (\gamma_s - \gamma_w)} \tag{3.19}$$

for the toe and channel bottom and

$$D_{50} = \frac{\tau_o}{0.04\ (\gamma_s - \gamma_w)} \tag{3.20}$$

for the channel side slopes where γ_s and γ_w are the specific weights of the stone and water, respectively. The same procedure can be used for bank protection. A graphic representation of Equation 3.19 is provided in Figure 3.4.

The Corps of Engineers Method was developed for channelized flows. Therefore, this procedure should be used to evaluate and/or design rock protection for the portions of the cover or embankment that are in the floodplain. This method is ideal for stabilizing cover and embankment toes.

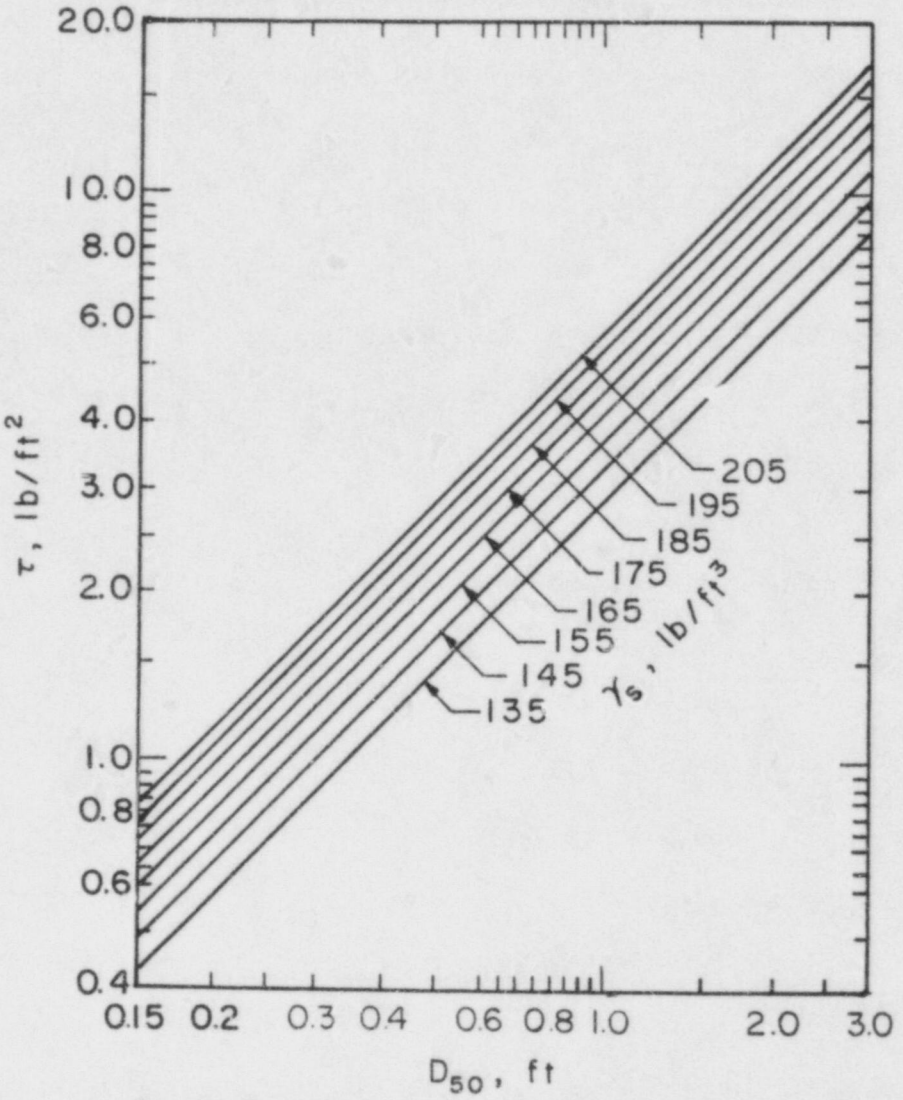

Basic Equation

$\tau = 0.040 (\gamma_s - \gamma_w) D_{50}$

where

τ = Design Shear Stress on Bottom of Channel

γ_s = Specific Weight of Stone

γ_w = Specific Weight of Water (62.4 lb / ft^3)

D_{50} = Theoretical Spherical Diameter of Average Size Stone

Fig. 3.4. Sizing of riprap as a function of design shear stress. Source: COE, 1970.

3.4.4 U.S. Bureau of Reclamation Method

The U.S. Bureau of Reclamation (USBR) Method (DOI, 1978) for riprap design was developed for the prevention of damage in and near stilling basins. The USBR procedure is empirically based upon extensive laboratory testing and field observations. Riprap failure was determined to occur because alternative design procedures underestimate the required stone size in highly turbulent zones, and there is a tendency for inplace riprap to be smaller and more stratified than specified. The USBR method is a velocity based design procedure.

Stone-Size Determination

The USBR method estimates the maximum stone size, D_{100}, as a function of the localized bottom velocity of flow, V_b, in feet per second. One means of predicting the maximum stone size is using the Mavis and Laushey (1948) procedure where

$$D_{100} = \left[\frac{V_b}{0.5\ (G_s - 1)^{0.5}} \right]^2 \qquad (3.21)$$

as D_{100} is the maximum stone size in mm and G_s is the particle specific gravity. If the bottom velocity can not be determined, local velocity may be substituted to size the rock. The local velocity can be determined using U.S. Army Corps of Engineers procedures (COE, 1970).

The stone size and stone weight can be determined from Figure 3.5 for a given bottom velocity, V_b. The resulting stone size is conservative. The riprap should be composed of a well-graded mixture of stone. Riprap should be placed on a filter blanket or bedding layer. The riprap layer should be 1.5 times as thick as the largest stone diameter. The filter blanket should be at least 6 inches thick.

It is recommended that the USBR method be considered only for design of rock along the toe-of-the-slope or where flow concentrations require substantial energy dissipation. This method would be well suited in areas where a hydraulic jump may occur. The USBR method is not necessarily recommended for bank and cover protection due to its conservatism.

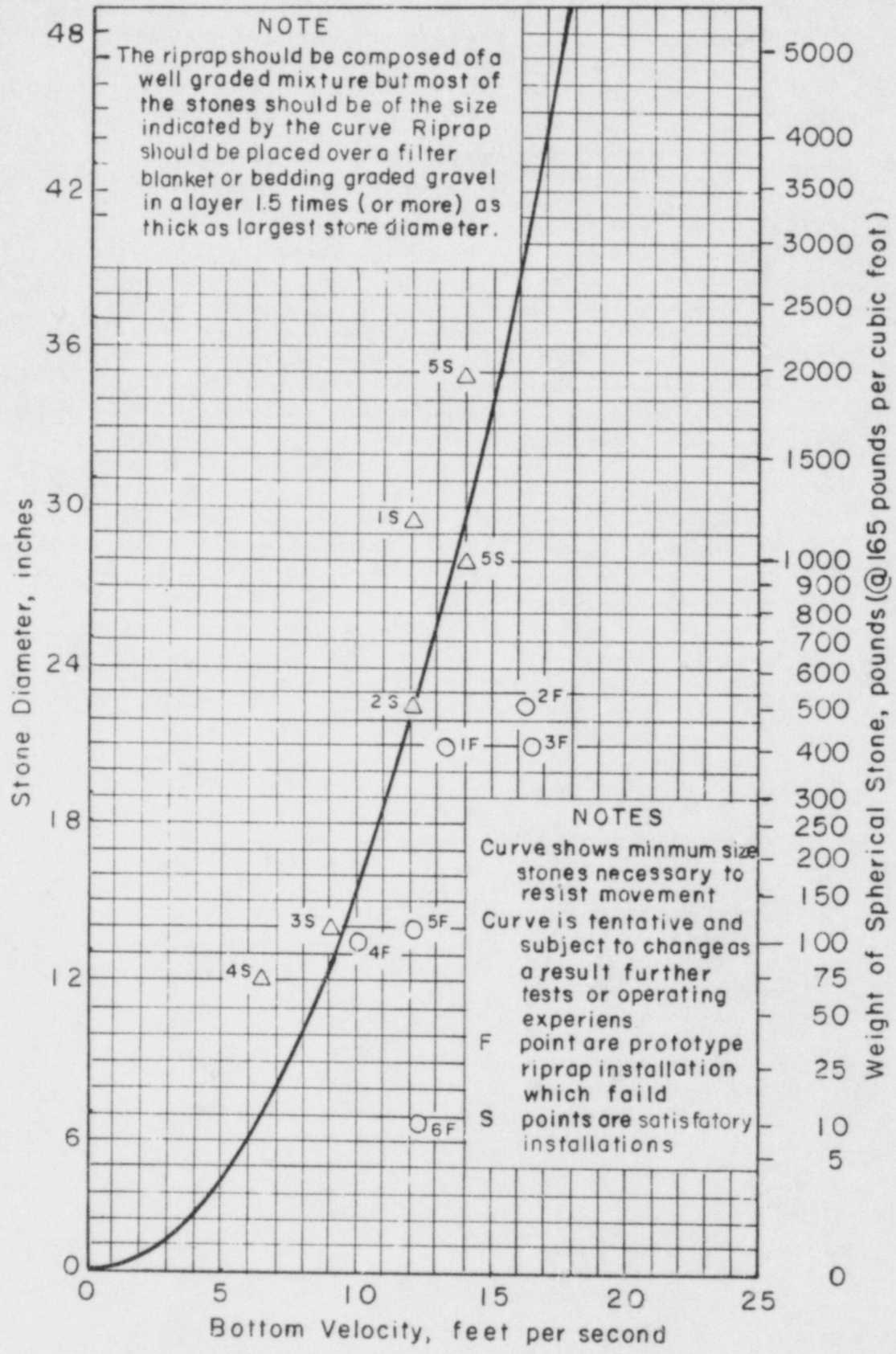

Fig. 3.5. Parametric curve used to determine maximum stone size in riprap mixture as a function of channel flow velocity.

4. RESULTS AND ANALYSIS

The study program concentrated on the acquisition of information related to identifying interstitial velocities in a rock layer, incipient rock movement, and riprap layer failure. To enhance the consistency of data acquisition, rock movement and riprap failure, criteria were determined prior to the beginning of experimentation.

Rock movement was observed during two distinct times of each test. Rock movement occurred when flow commenced and when the discharge was incrementally increased. During the change in discharge, the riprap layer appeared to settle and many of the individual stones moved to a more stable position. Rock movement and/or adjustment lasted only a few seconds. The riprap layer stabilization was not considered incipient movement of the stones resulting from the shear stresses and impinging flow. Incipient rock movement was determined after layer settlement occurred and when the force exerted by flow just overcame the resistance force of a particle to motion. Individual stones would initiate movement rolling over the rock layer.

The failure criterion of the riprap layer was when the filter blanket, or more often, the geofabric was exposed. In many cases, concentrated flows would scour a localized zone along the embankment. However, rock movement from up slope would subsequently fill and stabilize the scour area. When rock movement could no longer adequately replace the scour or failure zone, catastrophic failure was observed. Therefore, catastrophic failure occasionally occurred prior to filter cloth exposure due to the dynamic rock movement along the bed and due to poor conditions for observing the filter

resulting from the significant turbulence, bubbles, and air entrainment in the cascading flows.

4.1 FAILURE RELATIONSHIPS

The results are presented in Table 4.1 for 20 tests in the outdoor facility (12 ft) and in Table 4.2 for 32 tests in the indoor facility (8 ft).

As shown in Fig. 4.1, a family of curves were generated for slopes of 1 to 20% for median stone sizes ranging from 1 inch to 6 inches. The resulting unit discharges at failure (q_f) were dependent upon the stone size, D_{50}, and the slope. The results portrayed in Fig. 4.1 shall be referenced as the CSU relationship.

Experiment repeatability was a concern in establishing the CSU relationships presented in Fig. 4.1. Therefore, failure tests with no tailwater were repeated to verify the testing procedure and unit discharges at failure. The variance of unit discharges at failure were less than 10%.

It should be acknowledged that the CSU relationships presented in Fig. 4.1 are based on a relatively small data base. Verification of these relationships requires additional testing.

4.1.1 CSU-Stephenson Comparison

The relationship of median stone size and unit discharges at failure (q_f) presented in Fig. 4.1 were compared to the relationship derived by

Table 4.1. Summary of tests run in the outdoor flume (12 ft).[a]

Run No.	Riprap D_{50} Nominal (in.)	Riprap D_{50} Actual (in.)	Depth of Riprap (in.)	Depth of Filter (in.)	Slope of Embank.	Q (cfs)	q (cfs/ft)	V_{max}[b] (ft/s)	Placement of Riprap	Remarks
01	2	2.2	6	-	0.20	3.39	0.28[c]	3.70	Dumped	Rock movement and failure observed at st. 30 ft
01A	2	2.2	6	-	0.20	3.50	0.29[c]	2.90	Dumped	Complete slope failure
02	2	2.2	6	-	0.20	3.90	0.32[c]	-	Dumped	Complete slope failure
03	4	4.1	12	6	0.20	-	-	-	Dumped	Test run to measure velocity through rock
04	4	4.1	12	6	0.20	-	-	-	Dumped	Test run to measure velocity through rock
05	4	4.1	12	6	0.20	-	-	-	Dumped	Test run to measure velocity through rock
06	4	4.1	12	6	0.20	18.10	1.51	3.20	Dumped	Rock movement observed at st. 40 ft
07	4	4.1	12	6	0.20	21.78	1.81[c]	4.60	Dumped	Complete slope failure
08	5	5.1	12	6	0.20	-	-	-	Dumped	Test run to measure velocity through rock
09	5	5.1	12	6	0.20	26.19	2.18	-	Dumped	No rock movement
10	5	5.1	12	6	0.20	34.46	2.87	7.80	Dumped	Rock movement observed
10A	5	5.1	12	6	0.20	42.75	3.56[c]	-	Dumped	Complete slope failure

Table 4.1. Continued.

Run No.	Riprap D_{50} Nominal (in.)	Riprap D_{50} Actual (in.)	Depth of Riprap (in.)	Depth of Filter (in.)	Slope of Embank.	Q (cfs)	q (cfs/ft)	V_{max}[b] (ft/s)	Placement of Riprap	Remarks
11	6	6.2	12	6	0.20	-	-	-	Dumped	Test run to measure velocity through rocks
12	6	6.2	12	6	0.20	-	-	-	Dumped	Test run to measure velocity through rocks
13	6	6.2	12	6	0.20	31.10	2.59	-	Dumped	No rock movement observed
14	6	6.2	12	6	0.20	-	-	-	Dumped	Test run to measure velocity through rocks
15	6	6.2	12	6	0.20	53.12	4.43[c]	-	Dumped	Complete slope failure
16	2	2.2	6	6	0.20	-	-	-	Dumped	Test run to measure velocity through rock
17	2	2.2	6	6	0.20	5.58	0.46	3.30	Dumped	Rock movement observed
18	2	2.2	6	6	0.20	6.05	0.50[c]	3.50	Dumped	Complete slope failure

[a] All tests were run without tailwater.

[b] Maximum localized surface velocity.

[c] Indicates unit discharge at failure.

Table 4.2. Summary of tests runs in the indoor flume (8 ft).

Run No.	Riprap D_{50} Nominal (in.)	Riprap D_{50} Actual (in.)	Depth of Riprap (in.)	Depth of Filter (in.)	Slope of Embank.	Q (cfs)	q (cfs/ft)	V_{max}[a] (ft/s)	Placement of Riprap	Remarks
1	2	2.2	6	6	0.02	24.60	3.07	5.34	Dumped	No failure
2	2	2.2	6	6	0.02	48.60[d]	6.08[e]	7.33	Dumped	3 in. deep scour-failure
3	2	2.2	6	6	0.02	43.60	5.45	6.77	Dumped	No failure
4	2	2.2	6	6	0.02	46.90	5.87	6.87	Dumped	No failure
5	2	2.2	6	6	0.02	52.70	6.59	7.08	Dumped	No failure
6	2	2.2	6	6	0.02	56.60[d]	7.07[e]	7.07	Dumped	Exposure to filter material - failure
7[b]	2	2.2	6	6	0.02	36.00[d]	4.53[e]	6.12	Dumped	4 in. scour at the downstream end - failure
8	1	1.02	3	6	0.02	10.00	1.25	3.98	Dumped	No failure
9	1	1.02	3	6	0.02	15.20	1.90	4.60	Dumped	No failure
10	1	1.02	3	6	0.02	18.30	2.29[e]	4.87	Dumped	Exposure of filter material - failure
11[b]	1	1.02	3	6	0.02	8.85	1.11[e]	3.65	Dumped	1.9 in. scour at the downstream end - failure
12[c]	1	1.02	3	6	0.02	8.50	1.06	3.44	Dumped	No failure
13[c]	1	1.02	3	6	0.02	12.00	1.50	3.91	Dumped	No failure

Table 4.2. Continued.

Run No.	Riprap D_{50} Nominal (in.)	Riprap D_{50} Actual (in.)	Depth of Riprap (in.)	Depth of Filter (in.)	Slope of Embank.	Q (cfs)	q (cfs/ft)	V_{max}[a] (ft/s)	Placement of Riprap	Remarks
14[c]	1	1.02	3	6	0.02	15.00	1.88	4.35	Dumped	No failure
15[c]	1	1.02	3	6	0.02	17.80	2.23[e]	5.56	Dumped	Exposure of filter material - failure
16[c]	1	1.02	3	6	0.02	12.00	1.50	4.48	Dumped	No failure
17[c]	1	1.02	3	6	0.02	15.00	1.88	4.74	Dumped	No failure
18[c]	1	1.02	3	6	0.02	17.90	2.24[e]	5.37	Dumped	Exposure of filter material - failure
19[b]	1	1.02	3	6	0.01	10.00	1.25	3.07	Dumped	
20[b]	1	1.02	3	6	0.01	12.00	1.50[e]	3.22	Dumped	Exposure of filter material - failure
21	1	1.02	3	6	0.01	30.00[d]	3.75[e]	4.95	Dumped	2.6 in. scour at STA 150 - failure
22	1	1.02	3	6	0.01	35.00	4.37	5.03	Dumped	
23	1	1.02	3	6	0.01	40.00	5.00	5.40	Dumped	Max scour depth = 2.0 in. at STA 108
24	1	1.02	3	6	0.01	43.00	5.37[e]	5.40	Dumped	Exposure of filter material
25[b]	1	1.02	3	6	0.10	2.90	0.36[e]	-	Dumped	Exposure of filter material

Table 4.2. Continued.

Run No.	Riprap D_{50} Nominal (in.)	Riprap D_{50} Actual (in.)	Depth of Riprap (in.)	Depth of Filter (in.)	Slope of Embank.	Q (cfs)	q (cfs/ft)	V_{max}[a] (ft/s)	Placement of Riprap	Remarks
26[b]	1	1.02	3	6	0.10	2.70	0.34[e]	-	Dumped	Exposure of filter material
27[b]	1	1.02	3	6	0.10	2.48	0.31[e]	-	Dumped	Exposure of filter material
28[b]	1	1.02	3	6	0.10	3.35	0.42[e]	-	Dumped	Exposure of filter material
29[b]	2	2.20	6	6	0.10	9.00	1.12[e]	5.15	Dumped	Exposure of filter material
30[b]	2	2.20	6	6	0.10	10.00	1.25[e]	5.14	Dumped	Exposure of filter material
31[b]	2	2.20	6	6	0.10	10.00	1.25[e]	5.42	Dumped	Exposure of filter material
32[b]	2	2.20	6	6	0.08	14.50	1.81[e]	4.90	Dumped	Exposure of filter material

[a] Maximum localized surface velocity.
[b] Runs without tailwater.
[c] Runs without tailwater, the riprap in the last 3 ft of the downstream end of the test section was replaced by riprap of D_{50} = 2.5 in.
[d] Average discharge.
[e] Indicates unit discharge at failure.

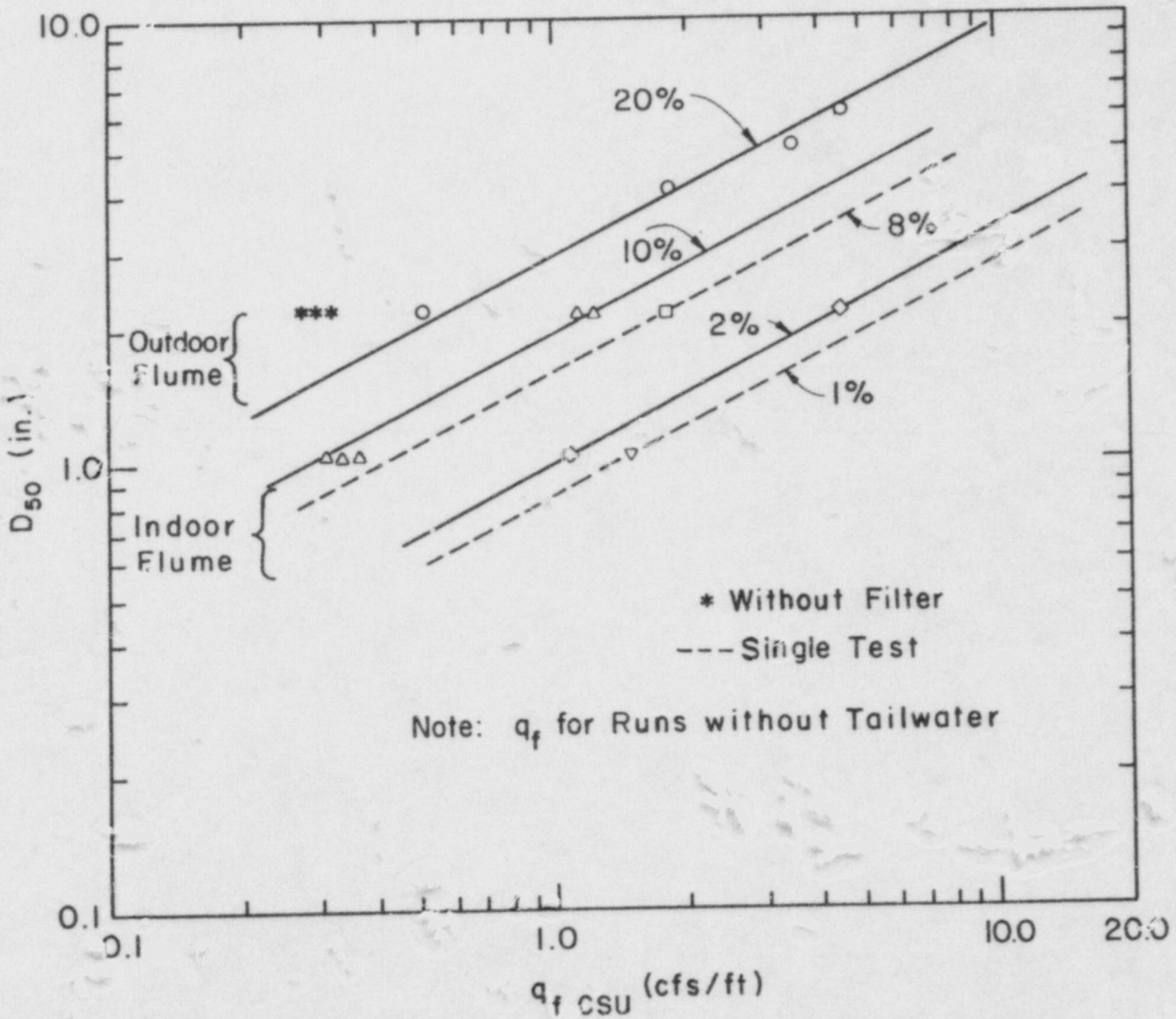

Fig. 4.1. Unit discharge and median stone size relationship at failure for CSU test data.

Stephenson (1979) for overtopping flows for rock-filled dams as presented in Eq. 3.15. Stephenson's relationship can be rearranged to estimate the threshold flow at which stone movement commences as

$$q_m^* = \frac{D_{50}^{3/2}\, C\, g^{1/2}\, [1-n_p)(G_s-1)\, \cos\theta\, (\tan\phi - \tan\theta)]^{5/3}}{(\tan\theta)^{7/6}\, n_p^{1/6}} \qquad (4.1)$$

where

q_m^* = unit discharge, threshold flow

D_{50} = median stone size

C = a constant equal to 0.22

g = gravitational acceleration

n_p = rockfill porosity

G_s = specific gravity

θ - angle of slope measured from horizontal

ϕ = angle of friction.

The unit discharge at failure, q_f^{**}, can be estimated by multiplying the unit discharge, q_m^*, computed in Eq. 4.1 by Oliviers' (Stephenson, 1979) constant.

$$q_f^{**} = q_m^* \times K \qquad (4.2)$$

where Oliviers' constant, K, is 1.20 for crushed gravel and 1.80 for crushed granite. Stephenson's unit discharge at failure and median stone size relationship is presented in Fig. 4.2 for 2%, 10% and 20% slopes.

To enhance a comparison of the CSU relationship presented in Fig. 4.1 with Stephenson's relationship presented in Fig. 4.2, the unit discharges at

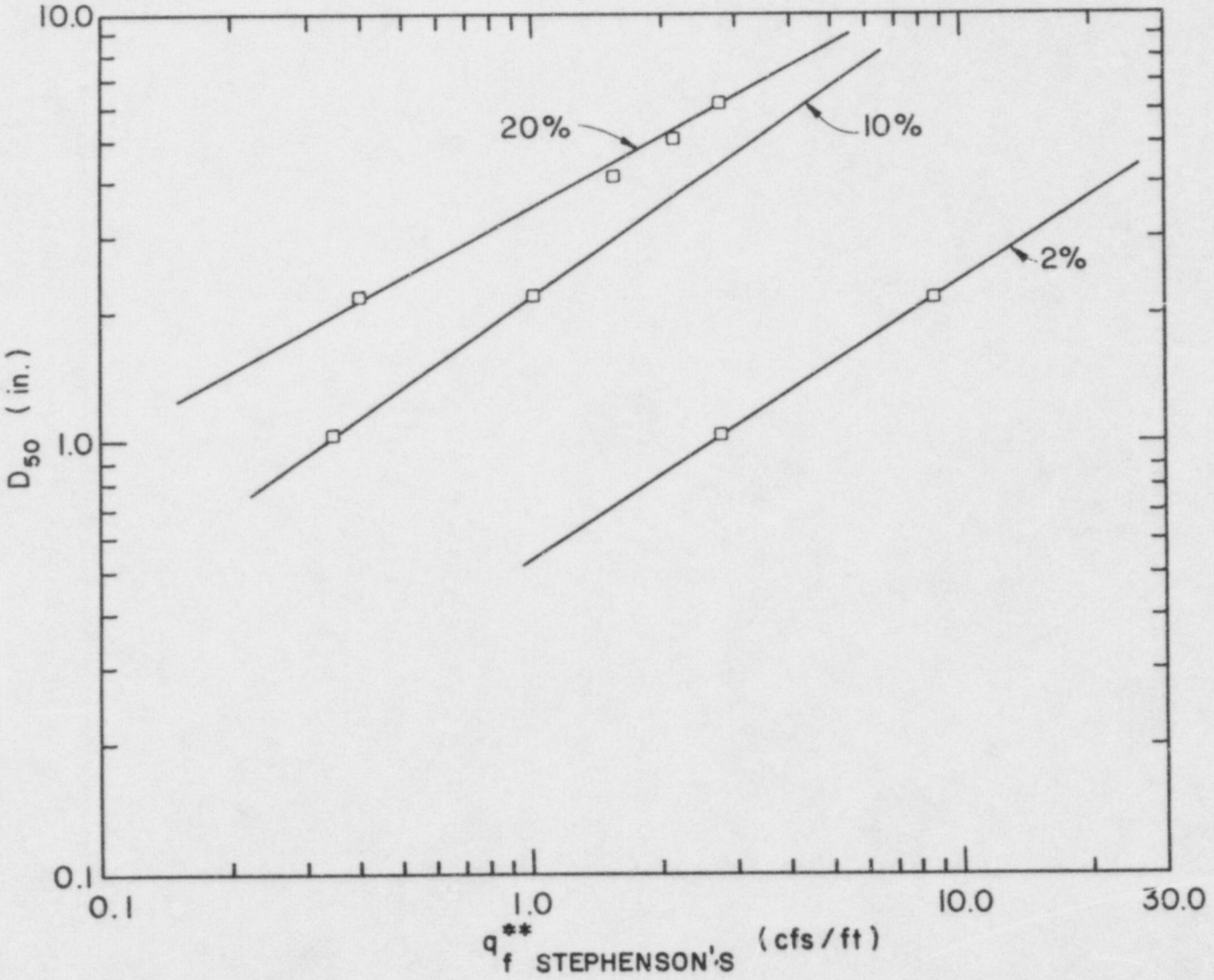

Fig. 4.2. Unit discharge and median stone size relationships at failure by Stephenson's Method (Stephenson, 1979).

failure were computed as presented in Table 4.3 and graphically presented in Fig. 4.3. It is observed in Fig. 4.3 that at a representative unit discharge of 1.0 cfs at failure, the Stephenson relationship yields a median stone size nearly 25% larger than does the CSU relationship for a 20% embankment slope. However, at a unit discharge of 1 cfs at failure for a 2% slope, the Stephenson relationship yields a median stone size nearly 42% smaller than the CSU relationship presented in Fig. 4.3. This comparison indicates that the Stephenson method for sizing riprap is an acceptable procedure for stabilizing reclaimed tailings embankments with slopes of 10% or greater. However, Stephenson's method does not yield a conservative median stone size for slopes under 10% and is not recommended for application to stabilizing reclaimed tailings covers.

4.1.2 Comparison of Riprap Design Methods

The CSU riprap design relationship presented in Fig. 4.1, developed for overtopping flows, was compared with the riprap design procedures presented by the U.S. Bureau of Reclamation (DOI, 1978), the U.S. Army Corps of Engineers (COE, 1970), the Safety Factors (SF) Method (Richardson et al., 1975), and the Stephenson (STEPH) Method (Stephenson, 1979). The unit discharge at failure and corresponding embankment slopes were extracted from Table 4.1 and Table 4.2 and used as input values for the CSU, USBR, COE, SF and STEPH design procedures and/or relationships. The calculated median stone diameters from each of these methods are presented in Table 4.4.

Table 4.3. Comparison of actual and theoretical discharge at failure.[a]

Run No.	Flume	Riprap D50 in. (Nominal)	Riprap D50 in. (Actual)	Slope	q_f (Actual Failure)	q_m^* (Theoretical Movement)	q_f^{**} (Theoretical Movement)
10	Indoor	1.00	1.02	0.02	2.29	2.30	2.67
06	Indoor	2.00	2.20	0.02	7.07	7.45	8.94
02	Outdoor	2.00	2.20	0.20	0.32	0.33	0.40
07	Outdoor	4.00	4.10	0.20	1.81	0.87	1.57
10A	Outdoor	5.00	5.10	0.20	3.55	1.20	2.16
15	Outdoor	6.00	6.20	0.20	4.43	1.52	2.74
18	Outdoor	2.00	2.20	0.20	0.50	0.33	0.40
25	Indoor	1.00	1.02	0.10	0.36	0.28	0.34
26	Indoor	1.00	1.02	0.10	0.34	0.28	0.34
27	Indoor	1.00	1.02	0.10	0.31	0.28	0.34
28	Indoor	1.00	1.02	0.10	0.42	0.28	0.34
29	Indoor	2.00	2.20	0.10	1.12	0.83	1.00
30	Indoor	2.00	2.20	0.10	1.25	0.83	1.00
31	Indoor	2.00	2.20	0.10	1.25	0.83	1.00
32	Indoor	2.00	2.20	0.08	1.81	1.30	1.56

[a] Definitions

q_f = actual flow (unit discharge) at failure in CSU tests

$$q_m^* = \frac{D_{50}^{3/2}\, C\, g^{1/2}\, [(1-n_p)(G_s-1)\cos\theta(\tan\phi - \tan\theta)]^{5/3}}{(\tan\theta)^{7/6}\, n_p^{1/6}}$$

= threshold flow (cfs/ft) at which movement of stone commences (Stephenson, 1979)

$q_f^{**} = q_m^* \times K$ = Unit discharge at failure (cfs/ft) by Oliviers' method (Stephenson, 1979)

K = Oliviers' constant, 1.20 for crushed gravel
1.80 for crushed granite

C = 0.22

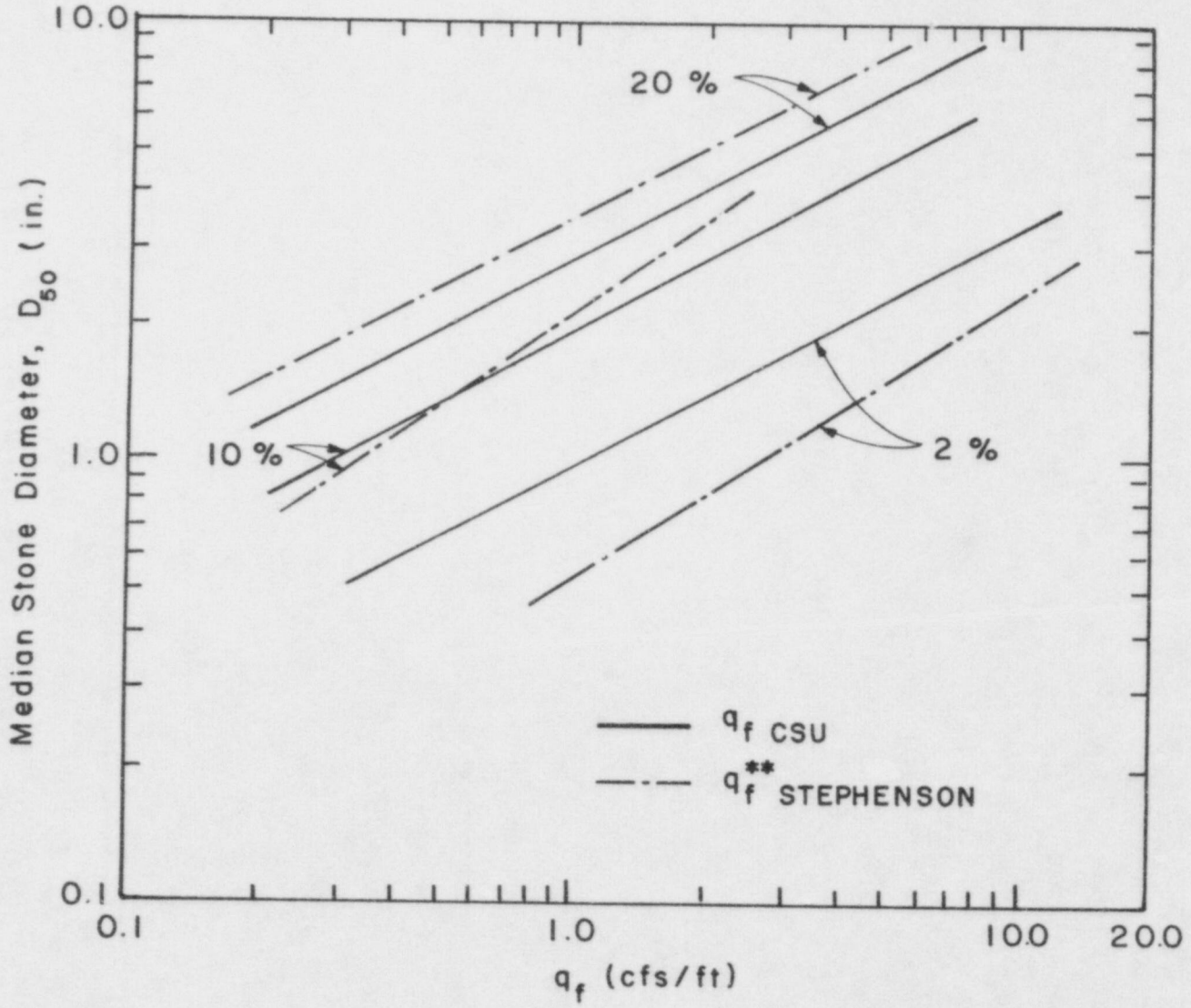

Fig. 4.3. Unit discharge and median stone size relationship at failure.

Table 4.4. Comparison of riprap sizing procedures.[a,b]

Run No.	Flume	Slope S	qf cfs/ft	D_{50} in. (CSU)	D_{50} in. (STEPH)	D_{50} in. (SF)	D_{50} in. (COE)	D_{50} in. (BOR)
20	Indoor	0.01	1.50	1.02	0.39	1.36	1.20	1.40
11	Indoor	0.02	1.10	1.02	0.69	1.77	1.20	1.75
25	Indoor	0.10	0.36	1.02	0.98	3.71	2.52	3.60
07	Indoor	0.02	4.50	2.20	1.39	3.00	2.16	5.25
31	Indoor	0.10	1.25	2.20	2.32	4.34	4.36	4.20
02[c]	Outdoor	0.20	0.32	2.20	1.90	2.36	4.36	--
18	Outdoor	0.20	0.50	2.20	2.56	2.75	6.00	--
07	Outdoor	0.20	1.81	4.10	4.51	6.40	6.60	5.00
10A	Outdoor	0.20	3.55	5.10	7.04	7.50	9.36	6.00
15	Outdoor	0.20	4.43	6.20	8.76	8.45	11.75	6.75

[a] All tests are for no tailwater condition.

[b] Definitions

D_{50} (CSU): Colorado State University test data.

D_{50} (STEPH): Stephenson, 1979.

D_{50} (SF): Richardson et al., 1975.

D_{50} (COE): COE, 1970.

D_{50} (BOR): BOR, 1978.

[c] Without filter bedding.

With the exception of the Stephenson Method at slopes of 2% and below, the various procedures generally yield a larger median stone diameter than does the CSU relationship (Table 4.4). For stone sizes of 4 to 6 inches, the COE procedure produces median stone diameters of 61% to 90% larger than the CSU relationship. Similarly, the SF and USBR procedures yield median stone diameters ranging from 36% to 56% and from 8% to 22%, respectively, larger than the CSU relationship. It is interesting to note that the Stephenson method yields a median stone size that is 41% larger than the CSU relationship at a 20% slope for a unit discharge at failure of 4.43 cfs.

The comparison indicates that for slopes of 10% and greater, the USBR, COE, SF and STEPH procedures yield conservatively larger stone sizes when applied to overtopping flow. It is acknowledged that the USBR and COE procedures were not developed for application to overtopping flows but rather for the stabilization of river banks and beds. The application of the COE, USBR, and SF riprap design procedures provide a conservative design for stabilizing tailings impoundments.

Conservatisms are important when engineers must provide designs that have extended lives of 200 to 1000 years. The conservatism accounts for many of the unknowns such as flow concentration, rock durability, water borne and wind borne sediments, and weathering. However, an overly conservative design will result in an escalation of stabilization costs. Therefore, the conservatism of the design must be carefully weighed against the additional costs of implementation.

4.2 INTERSTITIAL VELOCITIES

Velocity profiles of flow through the riprap layer were obtained for each stone size on each of the embankment slopes. Table 4.5 summarizes the velocity profiles for interstitial flow with the flow depth approximately at the riprap surface. Additional velocity profiles are presented in Appendix B.

4.2.1 Average Interstitial Velocity

An average interstitial velocity was calculated for each profile presented in Table 4.5 and plotted in Fig. 4.4. A unique relationship is observed for each embankment slope indicating velocity dependence on slope and median stone diameter. The CSU relationship was compared to the empirically derived Leps (1973) procedure for estimating interstitial flow velocities. The Leps relation is

$$V = \frac{Wm^{0.5}}{12} (i^{0.54}) \qquad (4.3)$$

where

V = velocty in feet per second

Wm = is an empirical constant

i = slope of the embankment.

Table 4.5. Velocity profiles for interstitial flows.

Run[a] No.	Flume	Riprap D_{50} (in.)	Depth of Riprap (in.)	Slope	Q_T (cfs)	Depth of Flow Relative to Riprap Surface (in.)	Velocity (ft/s) of Flow at Y inches Below Riprap Surface				Average Velocity (ft/s)	V_{Leps}[b] (ft/s)
							Y=1.5	Y=4.5	Y=7.5	Y=10.5		
6I	Indoor	1.02	3	0.01	0.11	0.00	0.10	--	--	--	0.10	0.08
7I	Indoor	1.02	3	0.02	0.11	0.00	0.13	--	--	--	0.13	0.12
9I[c]	Indoor	1.02	3	0.10	0.21	0.00	--	0.24	--	--	0.24	0.27
4I	Indoor	2.20	6	0.01	0.23	0.00	0.17	0.13	--	--	0.15	0.12
3I	Indoor	2.20	6	0.02	0.33	0.00	0.24	0.23	--	--	0.23	0.17
10I[d]	Indoor	2.20	6	0.10	0.56	0.00	0.36	0.36	--	--	0.36	0.40
11I[e]	Indoor	2.20	6	0.10	0.56	0.00	0.42	0.33	--	--	0.37	0.40
3[f]	Outdoor	4.10	12	0.20	4.34	0.00	0.69	0.82	0.81	0.56	0.72	0.85
4[g]	Outdoor	4.10	12	0.20	4.25	0.00	--	1.18	0.91	0.82	0.97	0.85
8[f]	Outdoor	5.10	12	0.20	5.70	0.00	--	0.86	1.11	1.15	1.04	0.93
8[g]	Outdoor	5.10	12	0.20	5.96	0.00	--	0.84	0.87	0.88	0.86	0.93
14[g]	Outdoor	6.20	12	0.20	6.22	0.00	--	--	--	--	--	--

a. Test runs 5, 15, 16, 1I, 2I, and 5I were not included due to malfunctioning equipment.
b Leps, 1973.
c Test run 9 at station 140-142.
d Test run 10 at station 140-142.
e Test run 11 at station 148-150.
f Test run at station 22-24.
g Test run at station 35-37.

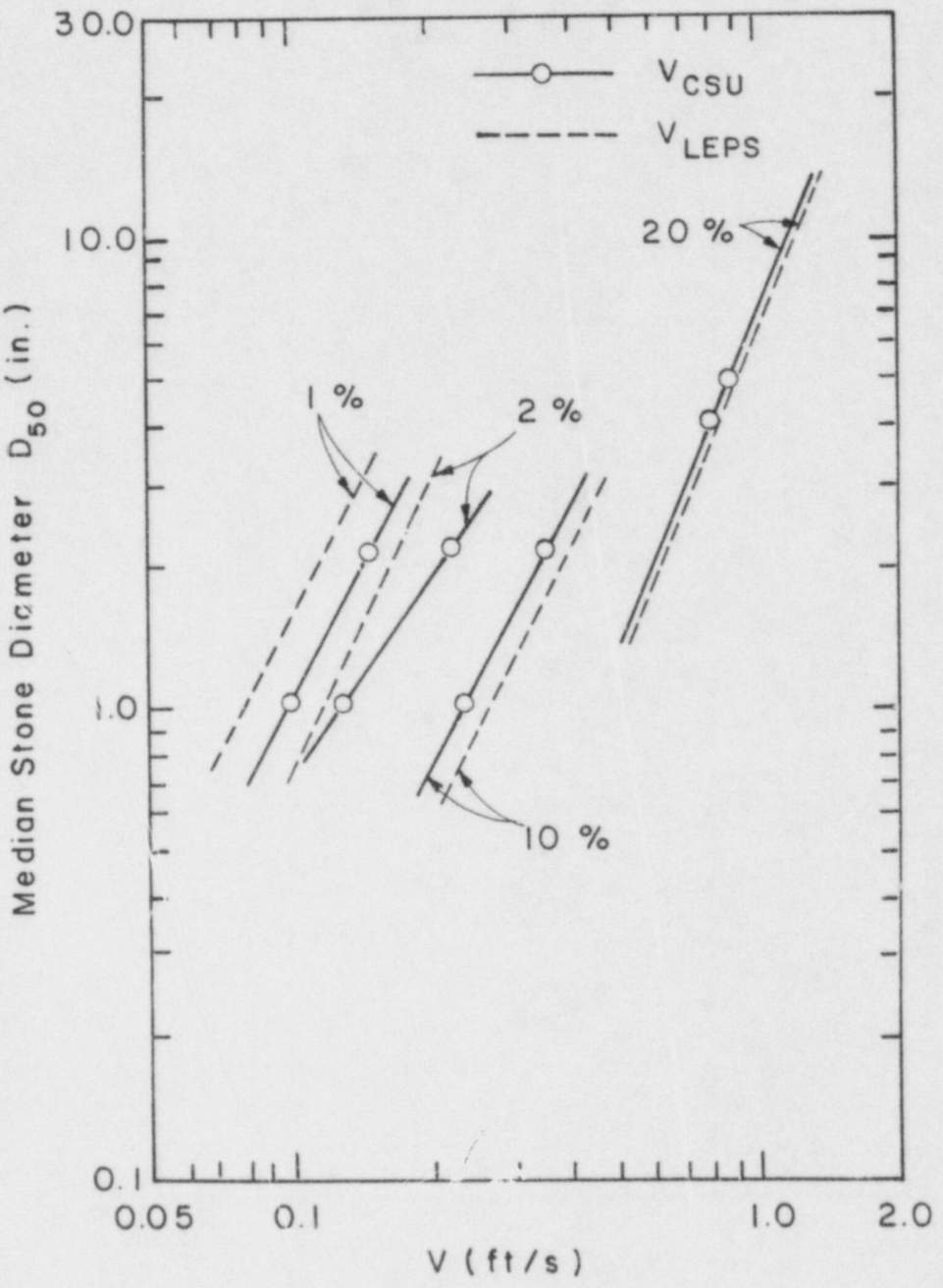

Fig. 4.4. Interstitial velocity relationships for CSU and Leps methods.

Median stone diameters and appropriate slopes were extracted from Table 4.5 and were calculated from Eq. 4.3. The resulting velocity relationships are presented in Fig. 4.4. It is observed that the CSU and Leps relationships are similar for slopes of 10% or greater. However, the CSU relationship yields higher interstitial flow velocities at slopes of 2% and less. Therefore, it is recommended that the Leps relationship be applied only to slopes of 10% or greater.

In an attempt to consolidate the CSU interstitial velocity relationships presented in Fig. 4.4, an analysis was conducted to evaluate the effect that riprap porosity, n_p, riprap coefficient of uniformity, C_u, median stone size, D_{50}, and embankment slope, S, have on the interstitial velocity. The dimensionless variables of stone porosity, coefficient of uniformity, and slope are graphically related to a dimensionless parameter comprising flow velocity, median stone diameter, and the acceleration of gravity in Fig. 4.5. The riprap properties and embankment slope effectively consolidated the data into a single relation expressed as

$$\frac{V}{(g\, D_{50})^{0.5}} = a\, C_u^b\, S^c\, n_p^d \qquad (4.4)$$

A multiple linear regression analysis was performed for Eq. 4.4 using the data in Appendix B. The coefficients resulting from this regression are:

a = 17.60

b = -0.074

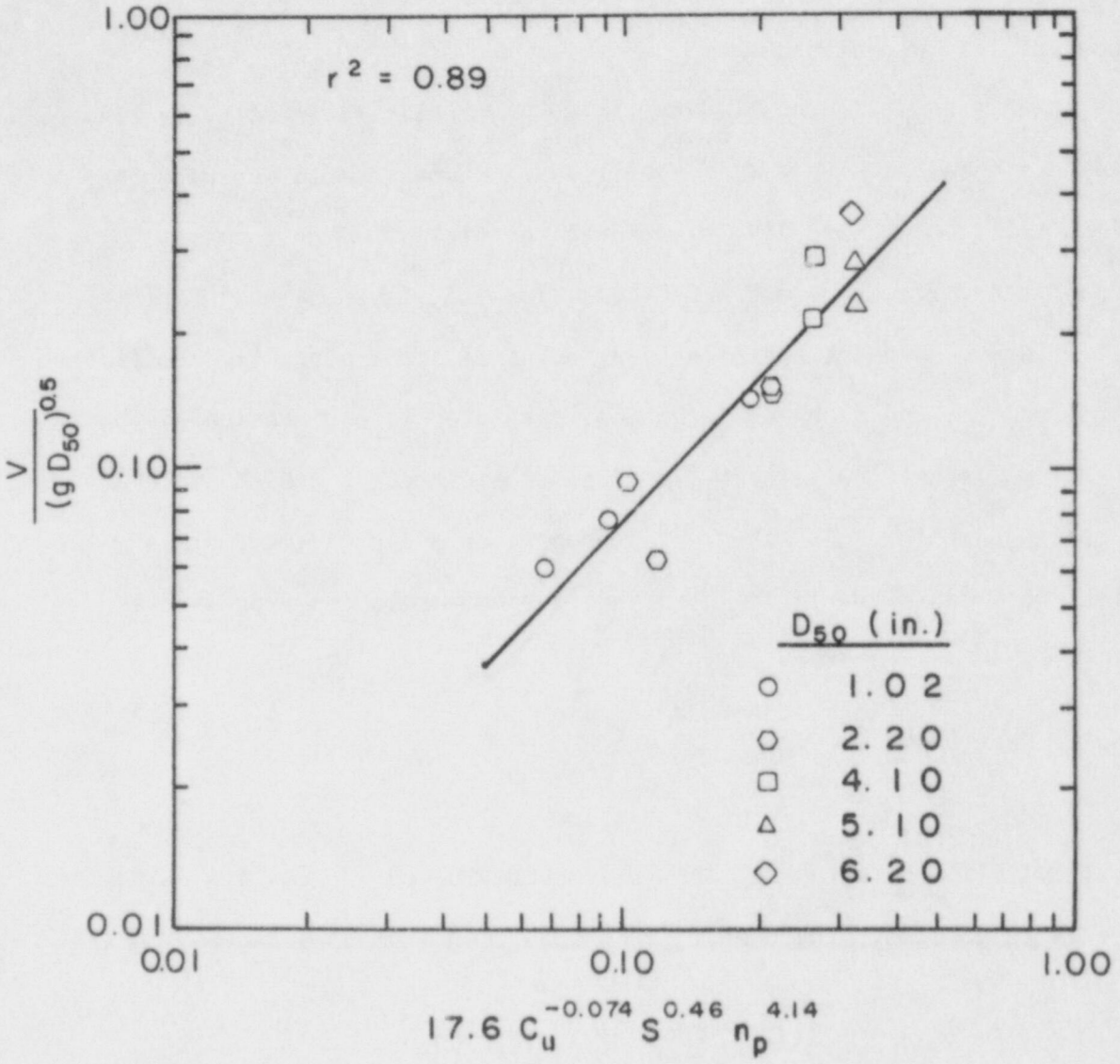

Fig. 4.5. Consolidated interstitial flow velocity relationship with CSU data.

$$c = 0.46$$

$$d = 4.14$$

Expressing the relationship of Fig. 4.5 in a power regression and solving Eq. 4.4 for velocity yields

$$V = 19.29 \left(C_u^{-0.074} S^{0.46} n_p^{4.14}\right)^{1.064} (g D_{50})^{0.5} \qquad (4.5)$$

Equation 4.5 allows the designer to estimate the interstitial flow velocity in the riprap layer as a function of the riprap properties and the embankment slope. The relationship in Eq. 4.5 was derived from riprap layer thicknesses of 3 inches to 12 inches. The correlation coefficient of the relationship presented in Fig. 4.5 is $r^2 = 0.89$.

4.2.2 Discharge Estimation for Unit Thickness

The riprap interstitial velocity relationship presented in Fig. 4.5 can be extended to estimate the unit discharge in the riprap layer. In order to incorporate a unit thickness term into the abscissa parameter of Fig. 4.5, the unit discharge, q, was modified to a unit discharge per inch of riprap thickness, q^*. The unit discharge was derived from the average velocity through the riprap layer with riprap thicknesses of 3 inches to 12 inches.

The parameter of unit discharge per unit thickness and median stone size was graphically correlated to the dimensionless variables of coefficient of uniformity, embankment slope, and porosity in Fig. 4.6.

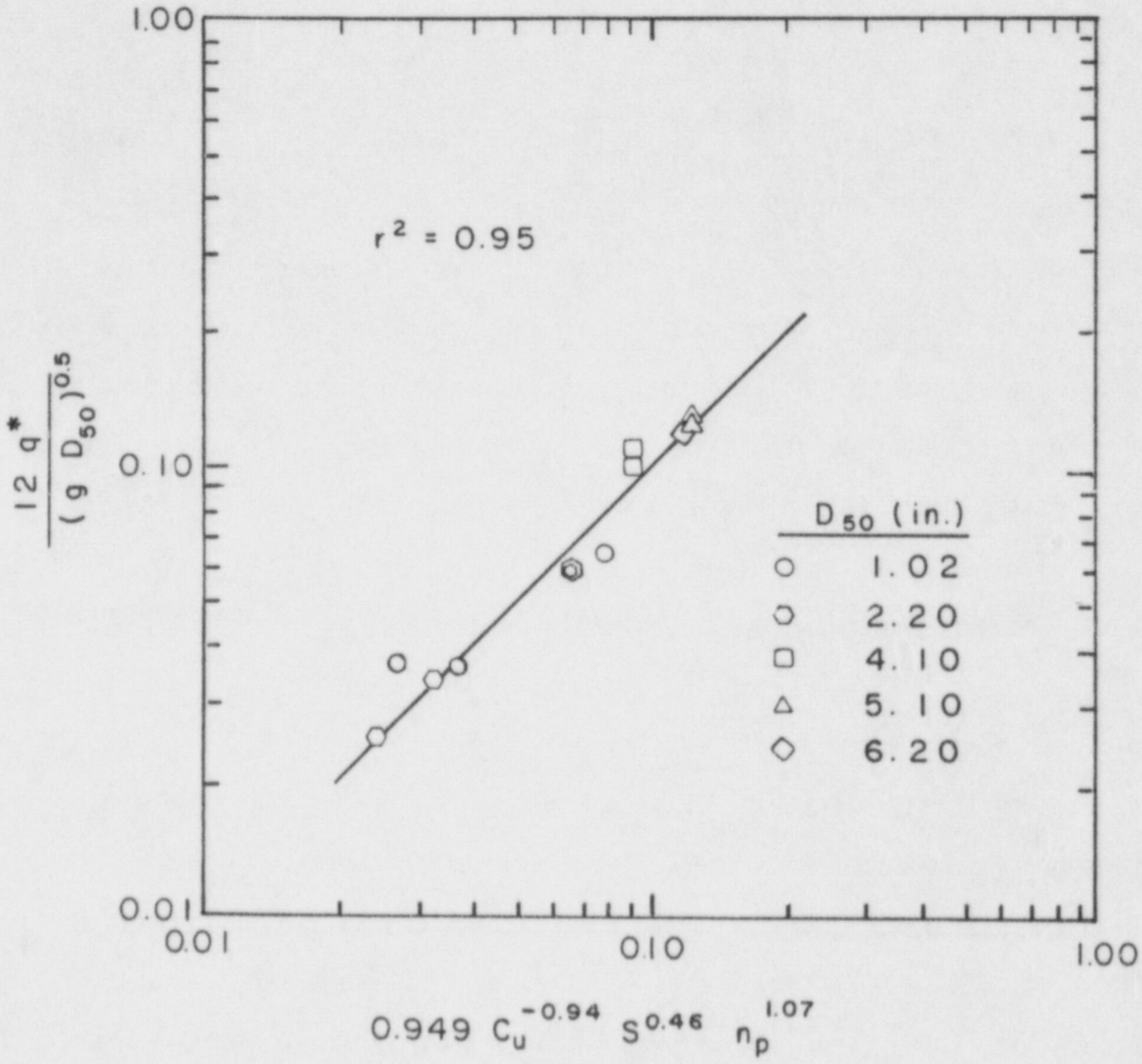

Fig. 4.6. Consolidated unit discharge per unit thickness with CSU data.

With the consolidated CSU data, this resulted in a single relationship that can be expressed as

$$\frac{12\ q^*}{(g\ D_{50})^{0.5}} = a\ C_u^b\ S^c\ n_p^d \qquad (4.6)$$

A multiple linear regression analysis was performed for Eq. 4.6. The coefficients resulting from this regression are:

a = 0.949

b = -0.94

c = 0.46

d = 1.07.

Expressing the relationship of Fig. 4.6 in a power regression and solving Eq. 4.6 for q^* yields

$$q^* = 0.079\ (C_u^{-0.94}\ S^{0.46}\ n_p^{1.07})^{0.999}\ (g\ D_{50})^{0.5} \qquad (4.7)$$

The correlation coefficient of the relationship presented in Fig. 4.6 is $r^2 = 0.95$.

4.3 RESISTANCE TO FLOW

The resistance to flow was estimated for each test condition using the data presented in Table 4.6 and 4.7 for the outdoor and indoor facilities,

Table 4.6. Resistance factors for tests run in the outdoor flume (12 ft).[a]

Run No.	D_{50} (in.)	Total Discharge Q_T (cfs)	Surface Discharge Q_s (cfs)	Slope S	Depth D=R (ft)	Velocity V (fps)	Area of Flow A (ft^2)	Froude Number F	Manning's n	Shields' Coefficient C_c	Reynold's Number Re	Darcy-Weisbach Friction Factor f
6	4.10	17.50	13.20	0.20	0.20	5.59	2.36	2.22	0.040	0.070	27270	0.324
7	4.10	21.78	17.48	0.20	0.22	6.62	2.64	2.49	0.037	0.078	28843	0.259
8	5.10	11.41	5.58	0.20	0.16	2.91	1.92	1.28	0.067	0.046	30597	0.976
9	5.10	26.19	20.36	0.20	0.26	6.53	3.12	2.26	0.041	0.074	39003	0.315
11	6.20	19.47	13.25	0.20	0.26	4.25	3.12	1.47	0.064	0.061	47416	0.743
12	6.20	19.80	13.58	0.20	0.23	4.92	2.76	1.81	0.051	0.054	44596	0.489
13	6.20	31.10	24.88	0.20	0.35	5.92	4.20	1.76	0.056	0.082	55013	0.514
17	2.20	5.58	4.14	0.20	0.10	3.45	1.20	1.92	0.041	0.066	10434	0.433
18	2.20	6.05	4.61	0.20	0.11	3.49	1.32	1.86	0.044	0.073	10944	0.465

[a] Definitions

$$F = \frac{Q_s/12}{(gD^3)^{0.5}}$$

$$n = \frac{1.486}{Q_s} D^{2/3} S^{1/2} A$$

$$V = \frac{Q_s}{A} \text{ (in ft/s)}$$

$$f = \frac{8gDS}{V^2}$$

$$A = 12 \times D \text{ (in ft}^2\text{)}$$

$$C_c = \frac{DS}{(G_s-1)\, D_{50}}$$

$$Re = \frac{D_{50}\,(gDS)^{0.5}}{\nu}$$

$$\nu = 1.41 \times 10^{-5} \text{ ft}^2/\text{s at } 50°F$$

Where, 'D' is the average of multiple readings shown in Appendix C.1.

Table 4.7. Resistance factors for tests run in the indoor flume (8 ft).[a]

Run No.	D_{50} (in.)	Total Discharge Q_T (cfs)	Surface Discharge Q_s (cfs)	Slope S	Depth D=R (ft)	Velocity V (fps)	Area of Flow A (ft^2)	Froude Number F	Manning's n	Shields' Coefficient C_c	Reynold's Number Re	Darcy-Weisbach Friction Factor f
1	2.20	24.60	24.27	0.02	0.57	5.34	4.56	1.26	0.025	0.038	11108	0.088
2	2.20	48.60	48.27	0.02	0.84	7.32	6.64	1.42	0.022	0.055	13404	0.066
3	2.20	43.60	43.27	0.02	0.81	6.77	6.48	1.33	0.024	0.055	13535	0.079
4	2.20	46.90	46.57	0.02	0.85	6.87	6.80	1.31	0.025	0.058	13932	0.081
5	2.20	52.70	52.37	0.02	0.93	7.08	7.44	1.29	0.025	0.063	14546	0.082
6	2.20	56.60	56.27	0.02	1.00	7.07	8.00	1.25	0.026	0.068	15076	0.086
7	2.20	36.00	35.67	0.02	0.74	6.12	5.92	1.25	0.026	0.050	12969	0.091
8	1.02	10.08	9.89	0.02	0.32	3.91	2.56	1.22	0.024	0.046	3859	0.100
9	1.02	15.20	15.09	0.02	0.41	4.60	3.28	1.26	0.024	0.060	4351	0.093
10	1.02	18.30	18.19	0.02	0.47	4.87	3.76	1.25	0.025	0.069	4642	0.094
11	1.02	8.90	8.79	0.02	0.30	3.65	2.40	1.17	0.025	0.045	3733	0.111
12	1.02	8.50	8.39	0.02	0.31	3.44	2.48	1.09	0.027	0.045	3764	0.128
13	1.02	12.00	11.89	0.02	0.38	3.91	3.04	1.11	0.027	0.056	4196	0.121
14	1.02	15.00	14.89	0.02	0.43	4.35	3.44	1.17	0.026	0.063	4445	0.109
15	1.02	17.80	17.69	0.02	0.42	5.30	3.36	1.44	0.021	0.060	4421	0.070
16	1.02	12.00	11.89	0.02	0.34	4.41	2.72	1.33	0.022	0.049	3977	0.083
17	1.02	15.00	14.89	0.02	0.40	4.74	3.20	1.33	0.023	0.058	4261	0.085
18	1.02	17.90	17.79	0.02	0.42	5.37	3.36	1.47	0.021	0.061	4372	0.069
19	1.02	10.00	9.89	0.01	0.41	3.07	3.28	0.85	0.025	0.029	3017	0.101
20	1.02	12.00	11.89	0.01	0.47	3.22	3.76	0.83	0.026	0.033	3228	0.104
21	1.02	31.70	31.59	0.01	0.80	4.95	6.40	0.98	0.023	0.057	4230	0.069
22	1.02	34.50	34.39	0.01	0.86	5.03	6.88	0.96	0.023	0.061	4378	0.070
23	1.02	40.00	38.89	0.01	0.94	5.40	7.52	0.98	0.023	0.067	4580	0.069
24	1.02	43.00	42.89	0.01	1.00	5.38	8.00	0.95	0.024	0.071	4823	0.071
26	1.02	2.70	2.49	0.10	0.08	4.10	0.66	2.49	0.022	0.059	4394	0.127
27	1.02	2.48	2.27	0.10	0.11	2.84	0.87	1.52	0.037	0.078	5039	0.339
28	1.02	3.35	3.14	0.10	0.14	2.98	1.14	1.37	0.043	0.102	5768	0.415
29	2.20	9.00	8.44	0.10	0.23	5.15	1.84	1.89	0.035	0.076	15777	0.234
30	2.20	10.00	9.44	0.10	0.25	5.00	2.00	1.76	0.036	0.083	16449	0.224

Table 4.7. Continued.

Run No.	D_{50} (in.)	Total Discharge Q_T (cfs)	Surface Discharge Q_S (cfs)	Slope S	Depth D=R (ft)	Velocity V (fps)	Area of Flow A (ft^2)	Froude Number F	Manning's n	Shields' Coefficient C_c	Reynold's Number Re	Darcy-Weisbach Friction Factor f
31	2.20	10.00	9.44	0.10	0.26	4.81	2.08	1.66	0.038	0.086	16775	0.272
32	2.20	14.50	13.94	0.08	0.35	5.18	2.80	1.54	0.038	0.093	17408	0.247

[a] Definitions

$$F = \frac{Q_T/8}{(gD^3)^{0.5}}$$

$$n = \frac{1.486}{Q_T} D^{2/3} S^{1/2} A$$

$$V = \frac{Q}{A} \text{ (in ft/s)}$$

$$f = \frac{8gDS}{V^2}$$

$$A = 12 \times D \text{ (in ft}^2\text{)}$$

$$C_c = \frac{DS}{(G_s-1) D_{50}}$$

$$Re = \frac{D_{50} (gDS)^{0.5}}{\nu}$$

$$\nu = 1.41 \times 10^{-5} \text{ ft}^2/\text{s at } 50°F$$

Where, 'D' is the average of multiple readings shown in Appendix C.2.

respectively. The values presented in Table 4.6 and 4.7 are averages of the individual data sets collected for each run. These average values better indicate data trends than do the individual data points from which these averages are derived. The individual data sets are presented in Table C.1 (outdoor flume) and Table C.2 (indoor flume) of Appendix C.

In the analysis, the Manning's roughness coefficient, n, the bed Shields' coefficient, C_c, and the Darcy-Weisbach friction factor, f, were computed using the equations presented in Chapter 3. Since the Manning's, Shields' and Darcy-Weisbach coefficients are interrelated, the analysis concentrates on the Manning's roughness coefficient.

One of the most difficult Manning's roughness values to determine is for riprap in cascading flow situations. The selection of an approximate n value is important to accurately depict the flow conditions needed to design a riprapped channel or embankment. The equation for calculating the Manning's roughness coefficient, n, is expressed as:

$$n = \frac{1.486}{Q_s} D^{2/3} S^{1/2} A \qquad (4.8)$$

where Q_s is the surface discharge, D is the depth of flow, S is the slope, and A is the cross-sectional area of flow. Other factors that affect Manning's roughness coefficient include surface roughness, channel irregularity, channel alignment, flow depth, silting and scouring, obstructions, and channel shape. Chow (1959) and Barnes (1967) present a comprehensive list of n values for open channel flow applications. Manning's n values commonly range from 0.017 for smooth channels to 0.07 for cobble bed streams.

4.3.1 Estimating Manning's n for Cascading Flow

The average Manning's roughness value, n, was computed for each failure test based on flow velocities and depths measured prior to failure, and are plotted versus the median stone size, D_{50}, in Fig. 4.7. It is observed in Fig. 4.7 that the n values for 1% and 2% slopes fall closely to the solid line representing a relationship developed by Anderson et al. (see Section 4.3.2). However, the n value for each stone size increased as the slope of the embankment increased, and the n value is over 40% higher when $Depth/D_{50} < 2$ (cascading flow conditions) than when $Depth/D_{50}$ is greater than 2 (Table 4.8).

A median stone size-slope parameter ($D_{50} \times S$) was correlated to the Manning's n value for the CSU data as presented in Fig. 4.8. Combining the median stone size and slope in one parameter appears to have reduced the data scatter. The relationship can be expressed as:

$$n = 0.0456 \, (D_{50} \times S)^{0.159} \qquad (4.8)$$

where D_{50} is in inches. The correlation coefficient, r^2, is 0.90. Therefore, a Manning's n value can be estimated for a riprapped surface in cascading flow as a function of the median stone size and slope.

4.3.2 Comparison of Procedures

A commonly used expression for determining Manning's n for riprap was presented by Anderson et al. (1970) as

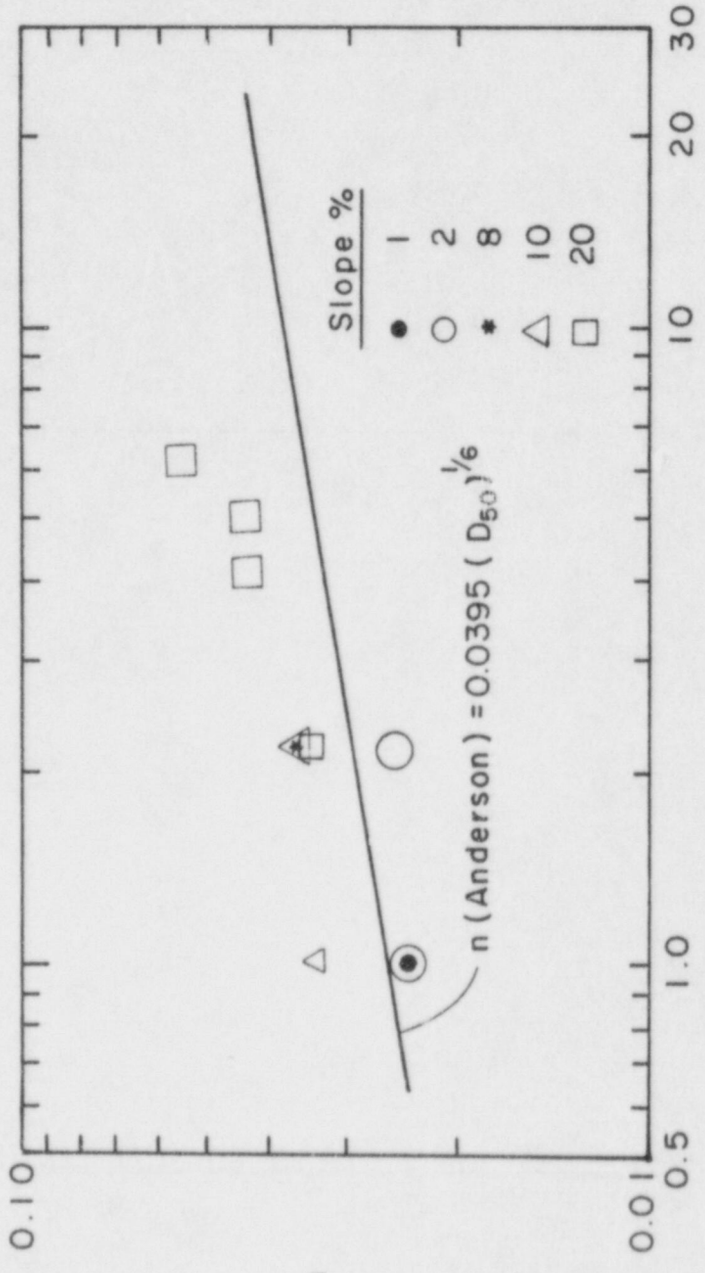

Fig. 4.7. Median stone diameter versus the Manning's n for CSU data.

Table 4.8. Summary of average Manning's n for CSU data.

D50 (in.)	D/D_{50}[a]	Slope	No. of Data Points	n_{CSU}
1.02	9.20	0.01	16	0.024
1.02	2.07	0.02	31	0.024
1.02	1.29	0.10	3	0.034
2.20	4.47	0.02	21	0.025
2.02	1.86	0.08	3	0.036
2.20	1.35	0.10	9	0.036
2.20	0.41	0.20	22	0.035
4.10	0.57	0.20	26	0.043
5.10	0.46	0.20	38	0.044
6.20	0.47	0.20	35	0.055

[a] Depth ÷ D_{50}

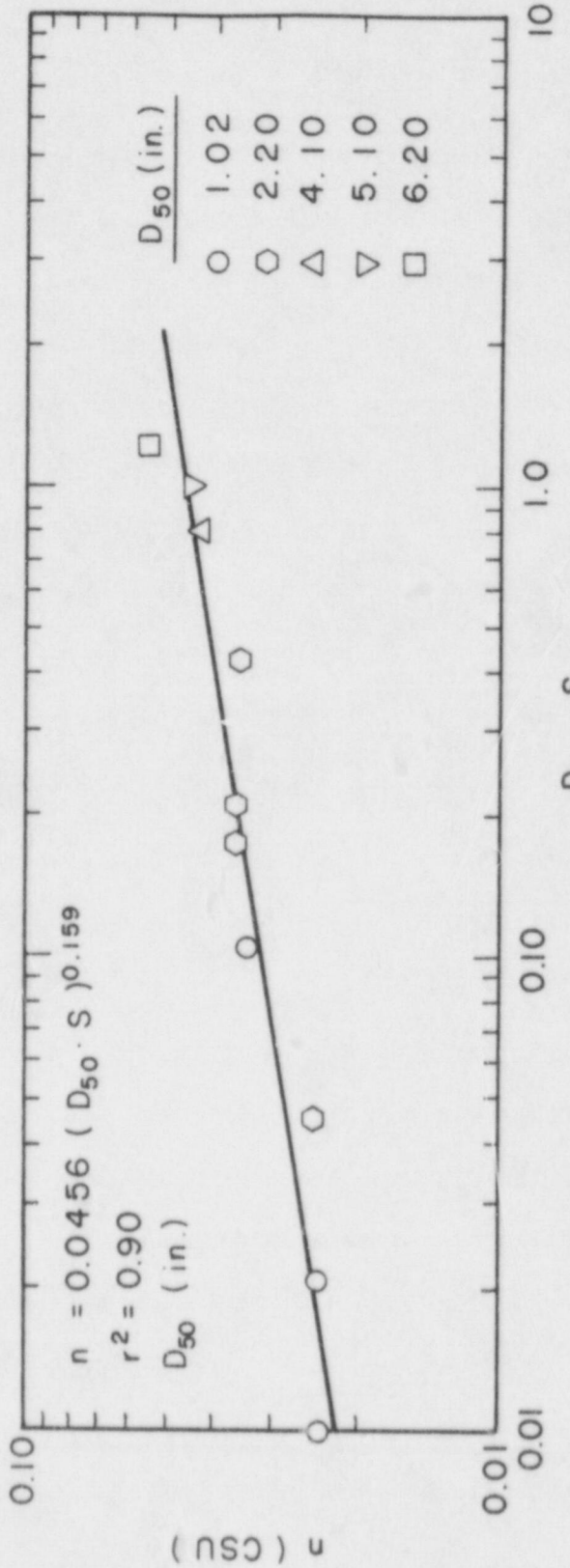

Fig. 4.8. Median stone size-slope parameter versus Manning's n for CSU data.

$$n = 0.0395\ (D_{50})^{1/6} \tag{4.9}$$

where D_{50} is the median stone size in feet. This relationship, which was developed from natural streams with slopes less than 2% for uniform flow conditions over submerged riprap is shown as the solid line in Fig. 4.7. However, the Anderson et al. (1970) relationship is commonly used and extrapolated to estimate roughness on steep slopes. Anderson et al. did not consider the resistance to be a function of slope.

The U.S. Army Corps of Engineers (COE, 1970) have also developed a procedure for estimating Manning's n value. Althrough the COE procedure was formulated for flat slopes and deep flow depths (1-60 ft), it is routinely applied to estimate flow resistance of steep slopes. The Manning's n is calculated as

$$n = \frac{R^{1/6}}{23.85 + 21.95 \log_{10} (R/K)} \tag{4.10}$$

where R is the hydraulic radius and K is the equivalent roughness height in ft. The equivalent roughness for stone lined channels is the theoretical spherical diameter of the median stone size. The hydraulic radius is approximated with the depth of flow in wide channels.

The CSU and Anderson et al. (1970) equations were compared to demonstrate the effect that slope has on the Manning's n. The Manning's n values were approximated by applying Eq. 4.8 and Eq. 4.9 for median stone sizes of 2.2 inches and 5.1 inches on slopes of 1%, 2%, 5%, 10% and 20%.

The results of the analysis (Table 4.9) indicate that at slopes below 2%, the Anderson et al. equation yields slightly greater n values (approximately 10%) than does the CSU equation. The CSU and Anderson et al. relations coincide at a slope between 2% and 5%.

The CSU and Anderson et al. relations yield significantly different Manning's n values at steep slopes ($\geq$10%). The Anderson et al. n value remains constant at 0.034 for a 5.1-inch stone (D_{50}) for all slopes. However, the CSU equation yields an n value of 0.046 for a 5.1-inch stone (D_{50}) at 20% slope, a value 35% greater than predicted by Anderson et al. It is evident that the Anderson et al. formulation can lead to erroneous designs if applied to slopes greater than 2%.

An attempt was also made to compare the Manning's n value from the U.S. Army Corps of Engineers procedure (COE, 1970) with the CSU results presented in Fig. 4.8. As observed in Table 4.9, the COE n values are less than the Anderson et al. and CSU values at slopes less than 10%. However, the COE value meets or exceeds the Anderson et al. and CSU n values for slopes of 10% or greater.

It should be noted that the CSU equation was based on computed average n values and does not indicate the upper range of localized n values which extended from 0.06 to 0.08. Appendix C, Summary of Hydraulic Data, presents the localized n values resulting from each test of the testing program.

4.3.3 Bed Critical Shields' Coefficient

The bed critical Shields' coefficient, C_c, was computed for each test as presented in Table 4.6 and Table 4.7. The Shields' coefficient of each

Table 4.9. Comparison of Manning's n.

D_{50} in.	Slope	$n_{(ANDER)}$ [a]	$n_{(COE)}$	$n_{(CSU)}$ [b]
2.2	0.01	0.030	--	0.025
2.2	0.02	0.030	0.025	0.028
2.2	0.05	0.030	--	0.032
2.2	0.10	0.030	0.029	0.036
2.2	0.20	0.030	0.044	0.040
5.1	0.01	0.034	--	0.028
5.1	0.02	0.034	--	0.032
5.1	0.05	0.034	--	0.037
5.1	0.10	0.034	--	0.041
5.1	0.20	0.034	0.047	0.046

[a] $n_{(ANDER)}$: Eq. 4.8.

[b] $n_{(CSU)}$: Eq. 4.9.

failure test, or average coefficient if more than one failure test was run, was determined for the flow just prior to failure for each stone size. The resulting coefficients were plotted on the Shields' Diagram (Simons and Senturk, 1977) as presented in Fig. 4.9. It is observed that the coefficients for the 1-inch, 2-inch, 4-inch, 5-inch, and 6-inch stone sizes failed just above the Shields' curve and significantly above Gessler's modification (Gessler, 1971). The riprap failure occurred with Shields' coefficients slightly greater than expected using the Shields' diagram. Therefore, the Shields' coefficient as presented in the Shields' diagram may be conservative for stone sizes of 1-inch or greater. Also, it is possible that the high Shields' coefficients reflect the slope influence of the bed.

4.4 TIME EFFECTS ON RIPRAP FAILURE

During the testing program, it was observed that the rising limb of the inflow hydrograph varied as a function of the time required to acquire data. Therefore it was necessary to analyze how the shape of the rising limb of the hydrograph affected the unit discharge at the failure of the riprap layer.

Three tests were conducted with the 2-inch riprap without filter on the 20% embankment slope. The unit discharge and test time in Table 4.10 are graphically presented in Fig. 4.10. It is observed in Fig. 4.10 that the time to failure in test No. 1 represents a steep rising limb of the inflow hydrograph while the time of failure in test No. 2 represents a slower, gradually rising limb. The unit discharges at failure are 0.28 cfs, 0.29 cfs and 0.31 cfs for tests No. 1, No. 1a and No. 2, respectively.

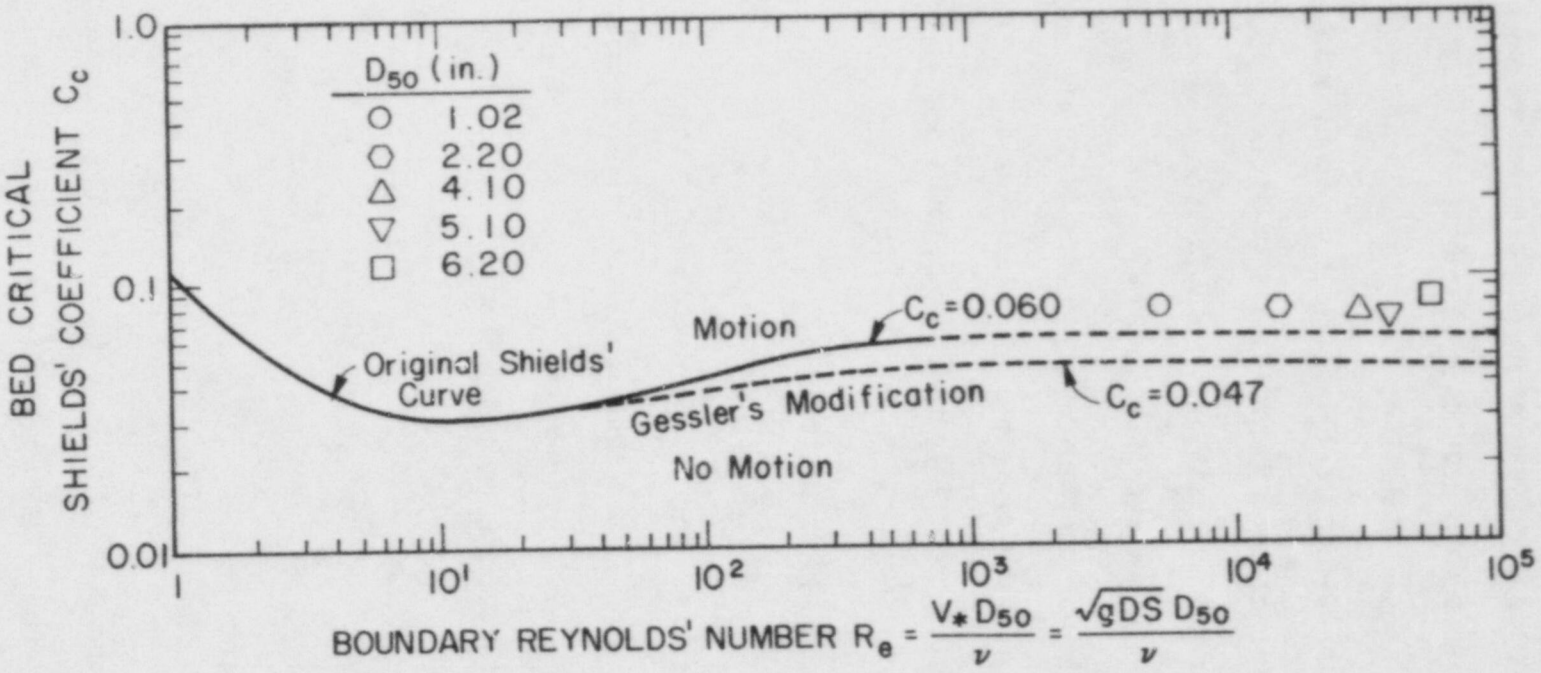

Fig. 4.9. Shields' diagram.

Table 4.10. Summary data for computing normalized time and discharge.[a]

Run No.	D_{50} (in.)	Slope	q (cfs/ft)	q_f (cfs/ft)	t (min)	t_f (min)	$\frac{q}{q_f}$	$\frac{t}{t_f}$
1	2.2	0.20	0.21	0.28	23	50	0.75	0.46
			0.28		50		1.00	1.00
1A	2.2	0.20	0.11	0.29	30		0.38	0.25
			0.15		65		0.52	0.54
			0.20		90		0.69	0.75
			0.29		12		1.00	1.00
2	2.2	0.20	0.13	0.32	75	150	0.40	0.50
			0.17		95		0.52	0.63
			0.20		115		0.61	0.77
			0.26		135		0.81	0.90
			0.28		145		0.86	0.97
			0.32		150		1.00	1.00
18	2.2	0.20	0.22	0.50	17	80	0.44	0.21
			0.32		27		0.64	0.34
			0.37		40		0.74	0.50
			0.50		80		1.00	1.00
7	4.1	0.20	0.72	1.81	40	150	0.40	0.27
			1.17		62		0.65	0.41
			1.40		90		0.77	0.60
			1.56		110		0.86	0.73
			1.72		139		0.95	0.93
			1.81		150		1.00	1.00
10A	5.1	0.20	0.91	3.56	57	193	0.26	0.29
			1.40		75		0.39	0.39
			1.57		98		0.44	0.51
			1.95		131		0.55	0.68
			2.45		157		0.69	0.81
			2.80		165		0.79	0.85
			2.87		183		0.81	0.95
			3.48		188		0.98	0.97
			3.56		193		1.00	1.00
15	6.2	0.20	1.44	4.43	20	63	0.32	0.32
			1.80		30		0.41	0.48
			2.63		47		0.59	0.75
			4.43		63		1.00	1.00

[a] Definitions

q = unit discharge at time 't'.
q_f = failure discharge.
t = time elapsed after starting the test.
t_f = total time of test.

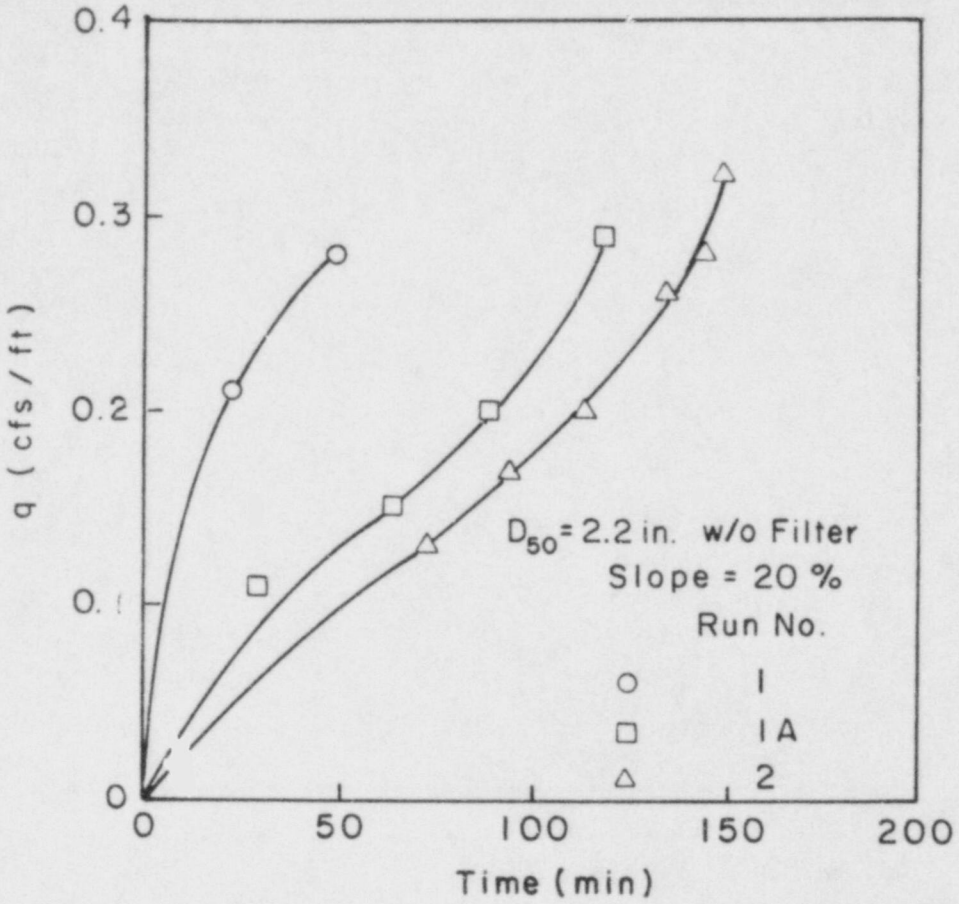

Fig. 4.10. Unit discharge versus time for 2-inch riprap at 20% slope.

It appears that the shape of the rising limb of the inflow hydrograph has little effect on the unit discharge at failure of the riprap layer as long as the flow does not exhibit dynamic wave loading conditions. However, if a ponding condition upstream of the riprap covered slope should suddenly burst, the riprap layer may fail at a lower unit discharge than reported in Section 4.1 due to unsteady, nonuniform flow conditions.

4.5 INCIPIENT STONE MOVEMENT AND CHANNELIZATION

4.5.1 Incipient Stone Movement

Incipient stone movement resulting from the force of the impinging flow was considered an important factor in determining the riprap failure criteria. The unit discharge was recorded during each test when stone movement was first observed. Stone movement was independent of bed settlement or shifting due to changes in the discharge. In each case, field observations were verified with the videotape recording of the test.

A graphical presentation of the normalized discharge versus the normalized time is presented in Fig. 4.11 for the 2-inch, 4-inch, 5-inch, and 6-inch stones with filter on a 20% embankment slope. It is observed that the stone movement occurred when the unit discharge approached approximately 76% $\pm$ 3% of the unit discharge at failure. The stone movement appears to be independent of the shape of the rising limb of the inflow hydrograph.

Therefore, stone movement unit discharge can be estimated as a function of the unit discharge at failure. Furthermore, incipient stone movement is

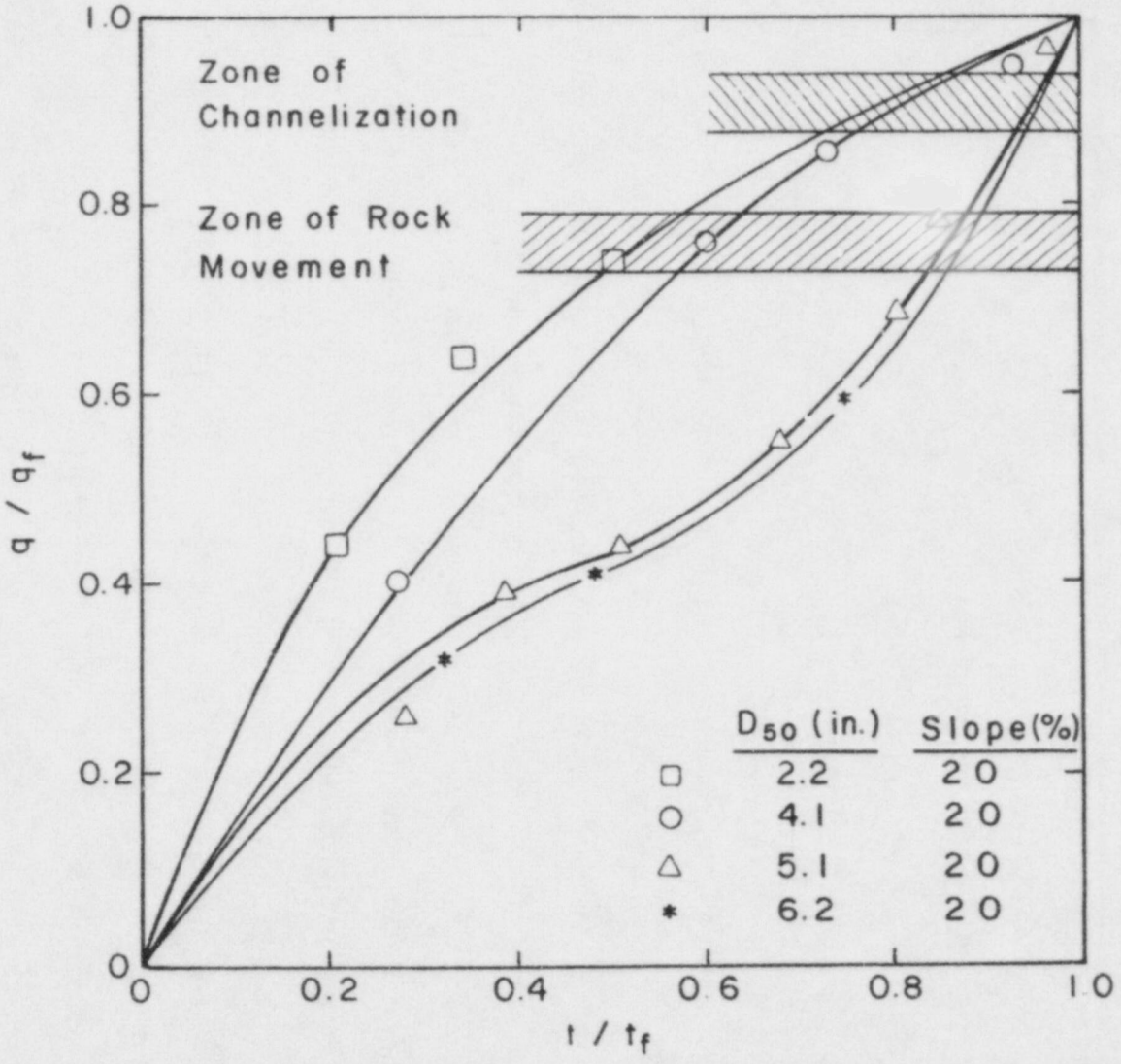

Fig. 4.11. Normalized unit discharge versus normalized time with filter.

independent of the shape of the hydrograph. These findings are based on a single slope and should be verified with additional tests on other slope(s).

4.5.2 Channelization

During several tests, small channels formed in the riprap layer conveying unit discharges greater than were expected under sheet flow conditions as previously indicated by Codell (1986). The channels appeared to form as flows were diverted around the larger stones and directed into areas or zones of the smaller stones. The smaller stones would move creating a gap or notch between the larger stones. The flow would concentrate into these notches thereby increasing the localized velocities and subsequently the local discharge. The newly formed channel would usually migrate downstream. However, migration often was across the embankment as well as directly down the embankment.

Although flow channelization was not well documented, evidence of channelization was obtained in four tests as summarized in Table 4.11. When channelization was observed, the channel depth and width were estimated and a localized velocity measurement was taken. The sheet flow unit discharge, q, was determined and compared to the unit discharge calculated from the localized channel, q_c. The ratio of q_c/q presented in Table 4.11 indicates that the channel may convey in excess of three times the discharge indicated for sheet flow conditions. It should be noted that the q_c/q ratio decreases as the stone size increases.

Table 4.11. Channelization of flow in the outdoor flume (12 ft).

Run No.	Riprap D_{50} in.	Q_T Total Flow cfs	Q Sheet Flow cfs/ft	Width of Channel ft	Depth of Channel ft	X-section Area of Channel ft^2	Velocity of Flow through Channel ft/s	Q_c Channel Flow cfs	q_c Rate of Flow through Channel cfs/ft	q_c/q	Q_c/Q	Concentration Factor $\frac{1}{1-Q_c/Q}$
01	2.2	3.36	0.28	2.50	0.25	0.63	3.70	2.33	0.93	3.33	0.69	3.23
02	2.2	3.36	0.28	3.00	0.33	0.99	1.90	1.88	0.63	2.24	0.56	2.27
07	4.10	21.72	1.81	4.00	0.58	2.32	5.20	12.06	3.02	1.67	0.56	2.27
10	5.10	33.48	2.79	3.00	0.50	1.50	7.80	11.70	3.90	1.40	0.35	1.54

In an attempt to quantify the degree of flow concentration that exists when channelization occurs, a flow concentration factor was formulated as

$$C_f = \frac{1}{1 - (Q_c/Q)} \tag{4.11}$$

where

C_f = Concentration factor

Q_c = Total channel discharge

Q = Total discharge.

The resulting concentration factor can be interpreted in at least two ways. The concentration factor can serve as an indicator of the "built-in" safety factor in the stability of the riprap design. The concentration factor could also be used as a multiplier or coefficient that may be integrated into a design procedure to increase stability against the unknown possibility of unsteady, nonuniform flow and subsequent channelization. The results are inconclusive because of the limited data base. However, it is evident that channelization can occur and is stone size dependent.

The videotape recordings of the failure tests were reviewed and the unit discharge at incipient channelization was documented. The incipient channelization unit discharges were normalized to the appropriate unit discharges at failure. The zone of incipient channelization is cross-hatched in Fig. 4.11. It is observed that incipient channelization occurs at approximately 90% $\pm$ 5% of the unit discharge at failure. Furthermore, the channelization appears to be independent of the shape of the inflow hydrograph.

4.6 FILTER INFLUENCE ON STABILITY

It is generally recommended that a filter blanket of well-graded rock material be placed over an embankment or cover prior to riprap placement. The filter blanket prevents migration of embankment or cover materials, acts to dissipate dynamic water forces between bedded layers, and stabilizes the riprap layer. The filter thickness varies depending upon the riprap stone size, riprap thickness, and riprap design procedure. Generally, a filter thickness of one-half the riprap layer thickness, but not less than 6 inches, is recommended.

The experimental program did not directly address how the filter blanket affected the stability of the riprap layers. However, one set of tests was conducted which indicates the potential effect of the filter blanket.

The 2-inch median stone diameter riprap was tested in the outdoor facility on a 20% slope with and without a 6-inch thick filter blanket. The average unit discharge at failure of the 2-inch riprap without a filter was 0.30 cfs/ft as presented in Fig. 4.1. However, when a 6-inch filter blanket was placed beneath the 6-inch layer of 2-inch riprap, the unit discharge at failure increased to 0.50 cfs/ft. Apparently, the presence of the filter increased the resistance to riprap movement by nearly 67%. The same riprap and method of riprap placement was used in all tests.

Several observations were made during and after each test. Because of the turbulence of the cascading flows on steep slopes, it was not possible to observe situations in which a "slow pumping" or extraction of the filter blanket may have occurred during each test. However, in several instances,

a cloud of filter material was observed in the flow just prior to the failure of the riprap layer. Also, a qualitative inspection of the unfailed portions of the embankment after each test indicated that the filter blanket often moved or adjusted with the riprap, but was not extracted from beneath the riprap layer.

Although the results do not provide sufficient evidence to support a final conclusion, the results indicate that the filter blanket may be a key element in the long-term stabilization of a riprap system. Furthermore, it is recommended that additional efforts be concentrated on the contributions of the filter blanket to the stability of the riprap system.

4.7 TOE STABILITY ON FLAT SLOPES

A series of tests were conducted with 1-inch riprap on 1% and 2% slopes to evaluate the tailwater effects on the riprap toe of the embankment. Also, the stability effect of oversizing riprap located at the toe of flat slopes was investigated.

The riprap stability on flat slopes was evaluated for both tailwater and no tailwater conditions. Unit discharges at failure were 1.50 cfs and 5.37 cfs for the no tailwater and tailwater conditions, respectively, for a 1% slope as presented in Table 4.2. Similarly, unit discharges at failure were 1.11 cfs for the no tailwater condition and 2.29 cfs for the tailwater condition at 2% slope. Therefore, the presence of tailwater increased the stability of the 1-inch and 2-inch riprap by 100% to 250% for these low slopes.

Since the design of flat slopes does not usually include a means of maintaining high tailwater, the effect of increasing the riprap stone size near the slope toe was investigated. The riprap median stone size was doubled in an attempt to stabilize the toe in a manner similar to a localized tailwater condition. The resulting unit discharge at failure for the no tailwater condition using 1-inch riprap at 2% slope was approximately 2.24 cfs. The unit failure discharge was 2.29 cfs for the same conditions with tailwater. Therefore, by doubling the median stone size placed near the toe of a flat slope ($S \leq 0.02$), the oversized riprap compensates for the low tailwater condition and serves to stabilize the toe.

5. CONCLUSIONS

A series of 52 laboratory experiments were conducted in which riprapped embankments were subjected to overtopping flows. Embankment slopes of 1, 2, 8, 10 and 20% were protected with riprap layers comprised of median stone sizes of 1, 2, 4, 5 and/or 6 inches. Riprap design criteria for overtopping flows were developed in terms of the unit discharge at failure, the interstitial velocities in the riprap layer, the resistance to flow over the riprap surface, the potential impacts of the filter blanket on riprap stability, and the effects of flow concentration on riprap stability. Specific findings are summarized as follows:

1. Rock Sizing
   - o A family of riprap design curves was developed from the CSU data relating unit discharge, embankment slope, and median stone size for overtopping flow when embankment slopes range from 1% to 20%.
   - o The Stephenson Method was determined to be an acceptable procedure for determining median stone diameter for overtopping flows with embankment slopes of 10% or greater.
   - o The COE, USBR, and SF design procedures for sizing riprap yield conservative median stone sizes for resisting overtopping flows.

Recommendations: The CSU, Stephenson, COE, USBR, and SF methods are acceptable procedures for sizing riprap to resist overtopping flows. However, it is not recommended that the Stephenson method be used for slopes less than 10%.

2. Interstitial Flows

   - o A procedure was derived from the CSU data to estimate interstitial velocities and discharges through a riprap layer as a function of the embankment slope, median stone size, coefficient of uniformity, and porosity.
   - o The Leps relationship for estimating interstitial velocities in a riprap layer should be applied only to slopes of 10% or greater.

Recommendation: The CSU and Leps methods are acceptable procedures for estimating interstitial velocities in riprap. However, the Leps method is not recommended for use on slopes under 10%.

3. Resistance to Flow

   - o The Manning's n was determined to be a function of the median stone size and slope in cascading flows.
   - o A relationship was presented that allows the user to estimate Manning's n for 1% to 20% slopes with median stone sizes from 1 inch to 6 inches.
   - o The CSU relationship yields higher n values than does the Anderson et al. or COE procedure for slopes less than 10%.

- o The Anderson et al. relation for determining n values should only be applied to channel or embankment slopes of 2% or less.
- o The bed critical Shields' coefficients, C_c, were determined to be more conservative than those values predicted by the Shields' diagram.

Recommendation: The CSU and Anderson et al. methods are acceptable procedures for estimating Manning's n values for slopes of 2% or less. The Anderson et al. relation should not be used for determining n values on slopes above 2%.

4. General Findings

- o The failure of the riprap layer was independent of the shape of the rising limb of the inflow hydrograph tributary to the embankment.
- o Incipient stone movement in the riprap layer occurred when the unit discharge approached 76% $\pm$ 3% of the unit discharge at failure.
- o Flow channelization occurred when the unit discharge approached 90% $\pm$ 5% of the unit discharge at failure.
- o The filter blanket stabilizes the riprap layer.
- o Tailwater stabilizes the riprap layer on slopes less than or equal to 2%.

Recommendation: Additional tests must be conducted to provide information indicating how the filter blanket stabilizes the riprap layer.

REFERENCES

Anderson, A. G., Paintal, A. S. and Davenport, J. T., 1970. Tentative Design Procedure for Riprap Lined Channels, Report No. 108, NCHRP.

Barnes, H. H., 1967. Roughness Characteristics of Natural Channels, Water-Supply Paper 1849, Geological Survey.

Chow, V. T., 1959. Open-Channel Hydraulics, McGraw-Hill Book Company.

Codell, R. B., 1986. Runoff from Armoured Slopes, Proc. from Geo-technical and Geo-hyrological Aspects of Waste Management, Colorado State University, Fort Collins, Colorado.

COE, 1970. Hydraulic Design of Flood Control Channels, EM 1110-2-1601, U.S. Army Corps of Engineers, July 1970.

COE, 1971. Engineering and Design, Additional Guidance for Riprap Channel Protection, ETL-1110-2-120, Office of the Chief of Engineers, U.S. Army Corps of Engineers, May 1971.

DOI, 1978. Hydraulic Design of Stilling Basins and Energy Dissipators, Engineering Monograph No. 25, Bureau of Reclamation, U.S. Department of the Interior.

Gessler, J., 1971. Beginning and Ceasing of Sediment Motion, River Mechanics, edited by H. W. Shen, Chapter 7, Fort Collins, Colorado.

Leps, T. M., 1973. Flow Through Rockfill, Embankment Dam Engineering, John Wiley and Sons.

Mavis, F. T., and Laushey, L. M., 1948. A Reappraisal of the Beginnings of Bed Movement-Competent Velocity, Proceedings of the International Association for Hydraulic Structures Research, Stockholm, Sweden.

Nelson, J. D., Abt, S. R., Hinkle, N. E., Staub, W. P., Volpe, R. L., and van Zyl, D., 1986. Methodologies for Evaluating Long-Term Stabilization Designs of Uranium Mill Tailings Impoundments, Phase I Report, NUREG/CR-4620, U.S. Nuclear Regulatory Commission, Silver Spring, MD, May 1986.

Richardson, E. V., Simons, D. B., Karaki, S., Mahmood, K., and Stevens, M. A., 1975. Highways in the River Environment - Hydraulics and Environmental Design Considerations, U.S. Department of Transportation. Available from Publications Office, Engineering Research Center, Colorado State University, Fort Collins, Colorado.

Ruff, J. F., Shaikh, A., Abt, S. R. and Richardson, E. V., 1985. Riprap Tests in Flood Control Channels, Prepared by Colorado State Uniersity for the U.S. Army Corps of Engineers, Waterways Experiment Station, Vicksburg, Mississippi, CER85-86JFR-AS-SRA-EVR17, August 1985.

Sherard, J. L., Richard, J. W., Stanley, F. G., William, A. C., 1963. Earth and Earth Rock Dams, John Wiley, 1963.

Simons, D. B. and Senturk, F., 1977. Sediment Transport Technology, Water Resources Publications, Fort Collins, Colorado.

Stephenson, D., 1979. Rockfill in Hydraulic Engineering, Developments in Geotechnical Engineering, 27, Elsevier Scientific Publishing Company, pp. 50-60.

APPENDIX A

RIPRAP AND FILTER GRAIN SIZE DISTRIBUTION

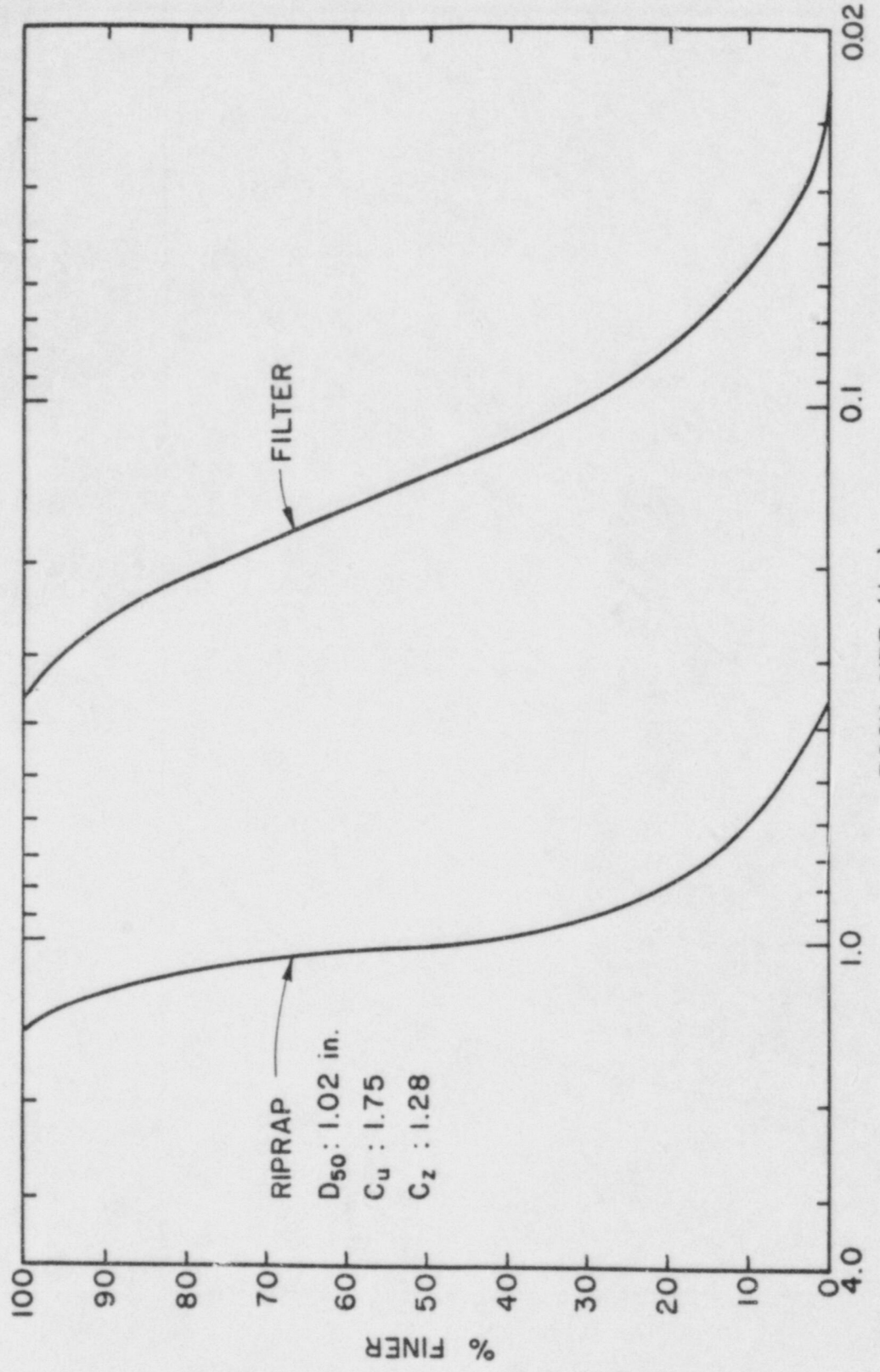

Fig. A.1. Grain-size distribution curve of 1.02 inch riprap.

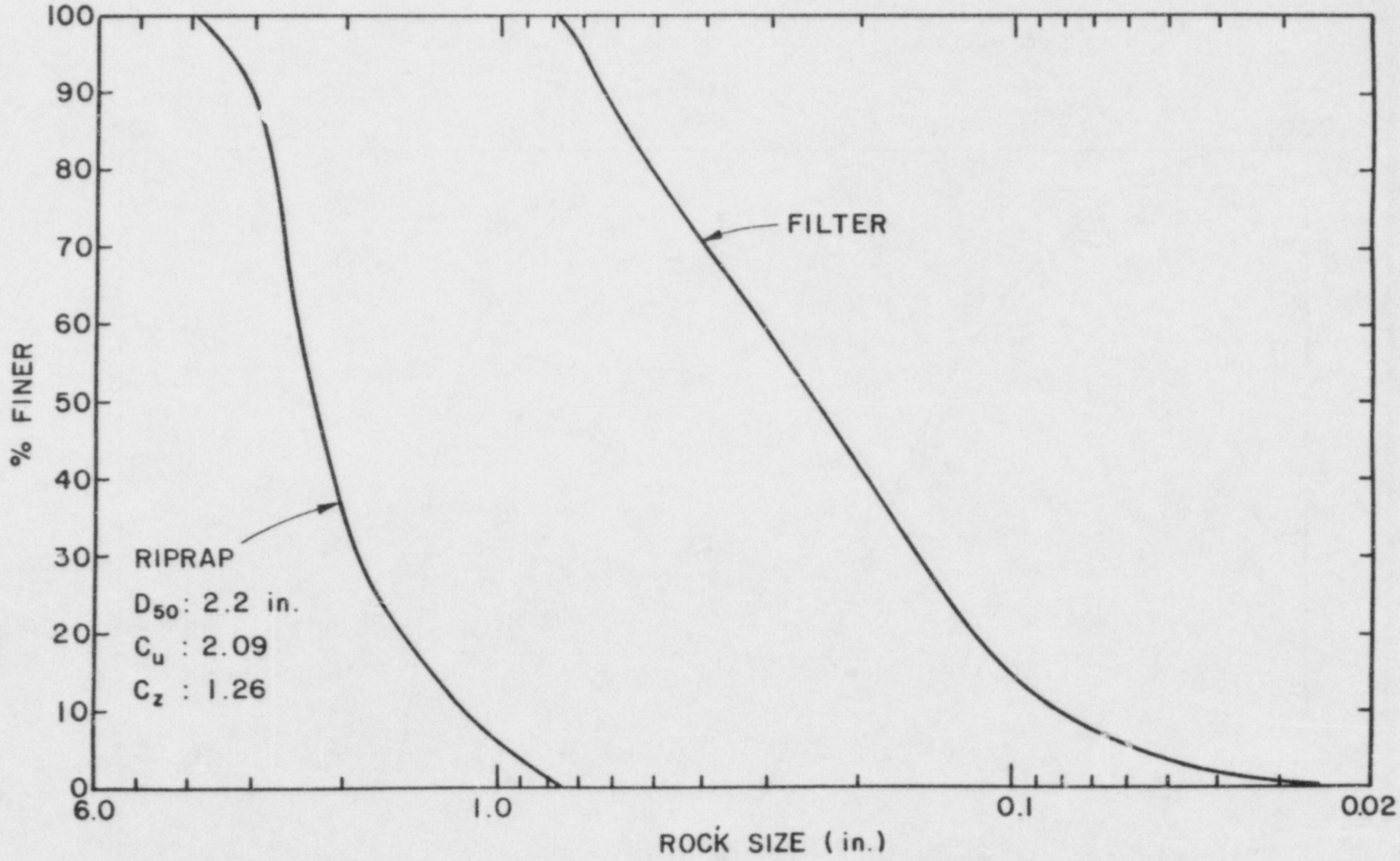

Fig. A.2. Grain-size distribution curve of 2.2 inch riprap.

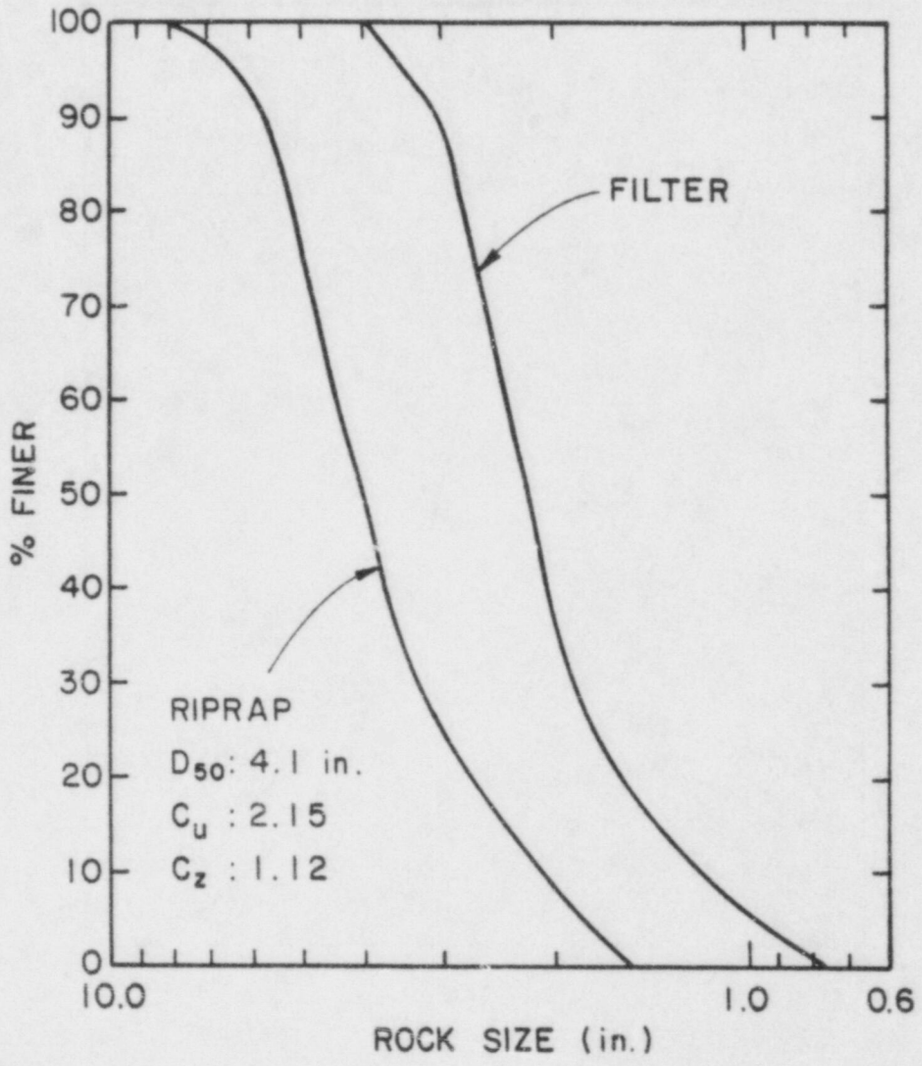

Fig. A.3. Grain-size distribution curve of 4.1 inch riprap.

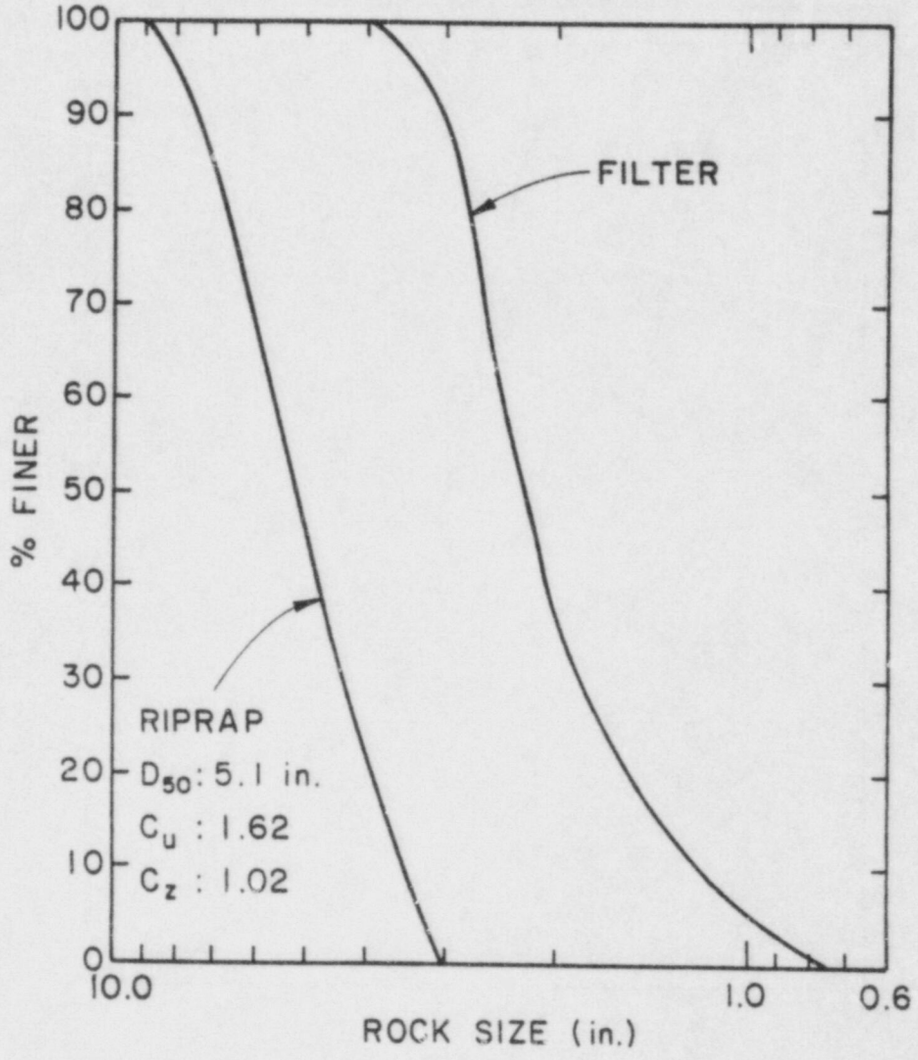

Fig. A.4. Grain-size distribution curve of 5.1 inch riprap.

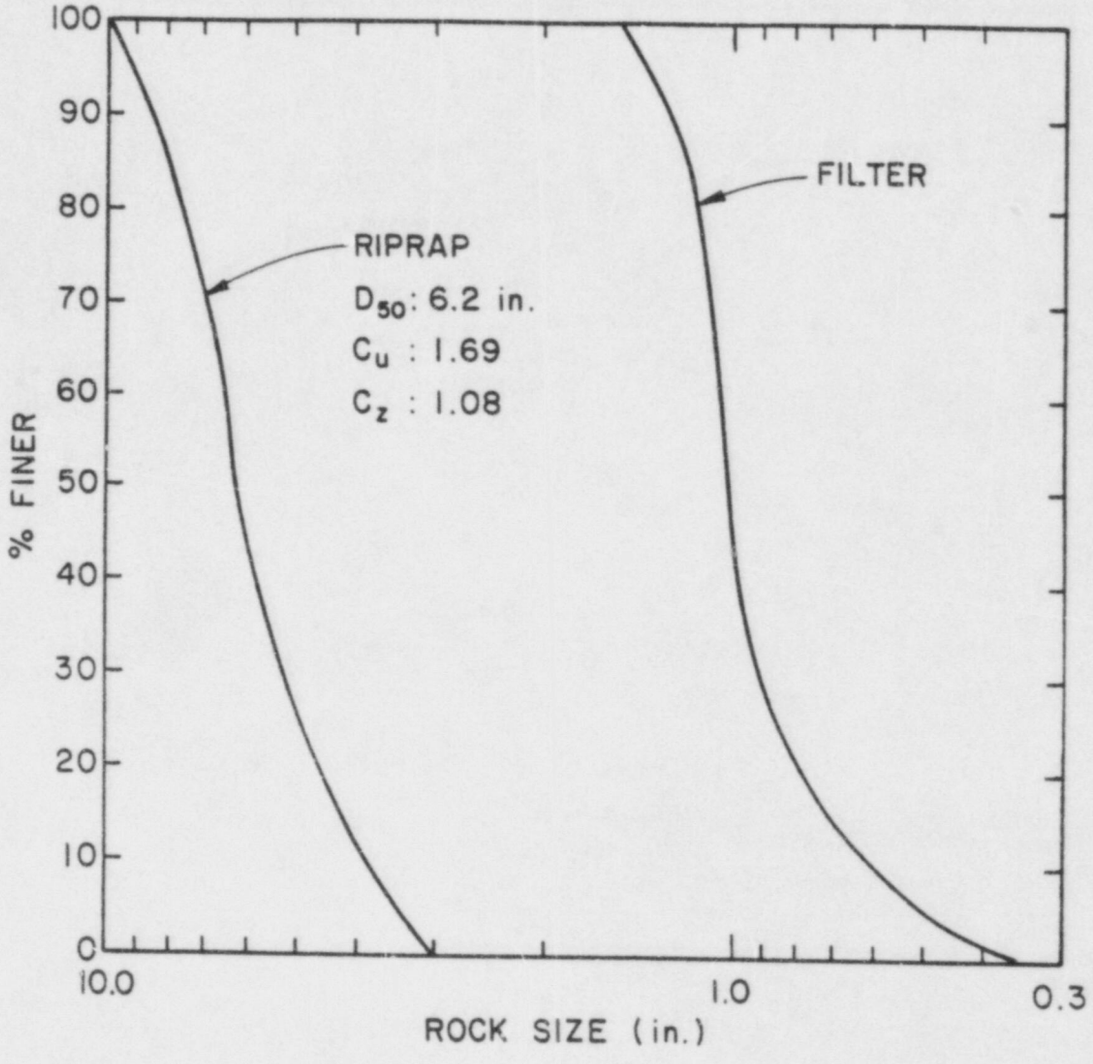

Fig. A.5. Grain-size distribution curve of 6.2 inch riprap.

APPENDIX B

INTERSTITIAL VELOCITY PROFILES FOR RIPRAP

Table B.1. Interstitial velocity and interstitial discharge for the outdoor flume (12 ft) and the indoor flume (8 ft).

Run[a] No.	Flume	Riprap D_{50} (in.)	Depth of Riprap (in.)	Slope S	Flume Width (ft)	Q (cfs)	q*[b] (cfs/ft/in.)	V[c] (ft/s)	C_u	n_p
6I	Indoor	1.02	3	0.01	8	0.11	0.0047	0.10	1.75	0.44
7I	Indoor	1.02	3	0.02	8	0.11	0.0047	0.13	1.75	0.44
9I	Indoor	1.02	3	0.10	8	0.21	0.0087	0.24	1.75	0.44
3I	Indoor	2.20	6	0.02	8	0.33	0.0067	0.23	2.09	0.45
4I	Indoor	2.20	6	0.01	8	0.23	0.0050	0.15	2.09	0.45
10I	Indoor	2.20	6	0.10	8	0.56	0.0120	0.36	2.09	0.45
11I	Indoor	2.20	6	0.10	8	0.56	0.0120	0.37	2.09	0.45
3[d]	Outdoor	4.10	12	0.20	12	4.34	0.0300	0.72	2.15	0.44
4[e]	Outdoor	4.10	12	0.20	12	4.25	0.0290	0.97	2.15	0.44
8[d]	Outdoor	5.10	12	0.20	12	5.70	0.0396	1.04	1.62	0.46
8[e]	Outdoor	5.10	12	0.20	12	5.96	0.0414	0.86	1.62	0.46
14[e]	Outdoor	6.20	12	0.20	12	6.22	0.0432	1.51	1.69	0.46

a Run 5, 15, and 16 outdoor and runs 1I, 2I, and 5I indoor were not included due to malfunctioning equipment.
b q* = unit discharge per inch depth of riprap.
c V = interstitial velocity.
d Test run at Station 22-24.
e Test run at Station 35-37.

Table B.2. Velocity profiles for interstitial flows in the outdoor flume (12 ft).

Run[a] No.	Riprap D_{50} (in.)	Slope	Depth of Riprap (in.)	Location of Test (Station)	Q_T (cfs)	Depth of Flow Relative to Riprap Surface (in.)	Velocity of Flow through Rocks at 'Y' inches below Riprap Surface (ft/s)			
							Y=10.5	Y=7.5	Y=4.5	Y=1.5
3	4.1	0.20	12	22-24	4.34	0.00	0.56	0.81	0.82	0.69
3	4.1	0.20	12	22-24	5.15	+0.70	0.54	0.82	0.83	0.71
3	4.1	0.20	12	22-24	8.00	+1.60	0.56	0.82	0.90	0.80
3	4.1	0.20	12	22-24	2.68	-4.60	0.55	0.77	--	--
4	4.1	0.20	12	35-37	4.25	0.00	0.82	0.91	1.18	--
4	4.1	0.20	12	35-37	5.31	+1.60	0.76	0.91	1.09	--
4	4.1	0.20	12	35-37	8.12	+2.85	0.73	0.99	1.06	1.82
4	4.1	0.20	12	35-37	2.58	-3.90	0.78	--	--	--
8	5.1	0.20	12	22-24	5.70	0.00	1.15	1.11	0.86	--
8	5.1	0.20	12	22-24	6.07	+0.70	1.03	1.02	1.10	--
8	5.1	0.20	12	22-24	8.75	+2.00	1.00	1.08	1.14	--
8	5.1	0.20	12	22-24	11.41	+3.00	1.08	1.23	1.39	--
8	5.1	0.20	12	22-24	2.90	-6.00	1.00	1.50	--	--
8	5.1	0.20	12	35-37	5.96	0.00	0.88	0.87	0.84	--
8	5.1	0.20	12	35-37	7.22	+1.00	--	0.90	0.86	--
8	5.1	0.20	12	35-37	9.74	+2.50	--	--	1.85	--
8	5.1	0.20	12	35-37	3.06	-6.00	0.66	0.84	--	--
14	6.2	0.20	12	35-37	4.58	-0.70	1.23	1.02	--	--
14	6.2	0.20	12	35-37	6.22	0.00	1.33	1.69	--	--
14	6.2	0.20	12	35-37	8.71	+1.40	1.36	1.36	1.85	--
14	6.2	0.20	12	35-37	10.75	+2.10	1.28	1.72	1.75	--
14	6.2	0.20	12	35-37	13.28	+2.60	1.16	1.61	1.78	--

[a] Runs 4, 5, 15, and 16 were not included due to malfunctioning equipment.

Table B.3. Velocity profiles for interstitial flows in the indoor flume (8 ft).

Run No.	Riprap D_{50} (in.)	Slope	Depth of Riprap (in.)	Location of Test (Station)	Q (cfs)	Depth of Flow Relative to Riprap Surface (in.)	Velocity of Flow through Rocks at 'Y' inches below Riprap Surface (ft/s)		
							Y=1.5	Y=4.5	Y=7.5
3I	2.20	0.02	6.0	120	0.33	0.00	0.23	0.24	--
3I	2.20	0.02	6.0	120	0.63	+0.85	0.24	0.26	--
3I	2.20	0.02	6.0	120	4.73	+3.00	0.23	0.28	--
3I	2.20	0.02	6.0	120	15.70	+5.90	0.26	0.66	--
3I	2.20	0.02	6.0	120	0.12	-3.00	0.19	--	--
4I	2.20	0.01	6.0	120	0.23	0.00	0.13	0.17	--
4I	2.20	0.01	6.0	120	0.63	+1.00	0.16	0.16	0.78
4I	2.20	0.01	6.0	120	3.74	+3.00	0.13	0.36	1.85
4I	2.20	0.01	6.0	120	12.40	+6.00	0.15	0.68	1.50
4I	2.20	0.01	6.0	120	0.07	-2.80	0.09	--	--
6I	1.02	0.01	3.0	120	0.11	0.00	0.10	--	--
6I	1.02	0.01	3.0	120	0.66	+1.00	0.09	--	--
6I	1.02	0.01	3.0	120	4.73	+3.00	--	1.89	--
6I	1.02	0.01	3.0	120	0.05	-0.80	0.10	--	--
7I	1.02	0.02	3.0	120	0.11	0.00	0.13	--	--
7I	1.02	0.02	3.0	120	6.26	+3.00	--	3.80	--
7I	1.02	0.02	3.0	120	13.60	+4.80	--	3.60	--
7I	1.02	0.02	3.0	120	0.04	-1.40	0.11	--	--
8I	1.02	0.02	3.0	120	0.08	0.00	0.11	--	--
8I	1.02	0.02	3.0	120	0.66	+1.00	0.09	--	--
8I	1.02	0.02	3.0	120	4.73	+2.80	--	1.60	--
8I	1.02	0.02	3.0	120	9.46	+4.00	--	2.24	3.20
8I	1.02	0.02	3.0	120	0.01	-1.40	0.09	--	--

Table B.3. Continued.

Run[a] No.	Riprap D_{50} (in.)	Slope	Depth of Riprap (in.)	Location of Test (Station)	Q (cfs)	Depth of Flow Relative to Riprap Surface (in.)	Velocity of Flow through Rocks at 'Y' inches below Riprap Surface (ft/s)		
							Y=1.5	Y=4.5	Y=7.5
9I	1.02	0.10	3.0	140-142	0.21	0.00	0.24	--	--
9I	1.02	0.10	3.0	140-142	0.40	+0.95	0.24	--	--
9I	1.02	0.10	3.0	140-142	0.67	+1.28	0.31	--	--
9I	1.02	0.10	3.0	140-142	1.67	+1.67	0.17	--	--
9I	1.02	0.10	3.0	140-142	0.10	-1.73	0.17	--	--
10I	2.20	0.10	6.0	140-142	0.56	0.00	0.36	0.36	--
10I	2.20	0.10	6.0	140-142	0.68	+0.17	0.37	0.37	--
10I	2.20	0.10	6.0	140-142	2.12	+1.25	0.36	0.38	--
10I	2.20	0.10	6.0	140-142	5.02	+2.11	0.36	0.35	--
10I	2.20	0.10	6.0	140-142	0.29	-2.93	0.33	--	--
11I	2.20	0.10	6.0	148-150	0.56	0.00	0.33	--	--
11I	2.20	0.10	6.0	148-150	0.67	+0.40	0.36	0.39	--
11I	2.20	0.10	6.0	148-150	2.12	+1.05	0.34	0.41	0.83
11I	2.20	0.10	6.0	148-150	5.02	+2.15	0.35	0.36	1.06
11I	2.20	0.10	6.0	148-150	0.29	-2.40	0.32	--	--

[a] Run 1I, 2I, and 5I were not included due to malfunctioning equipment.

APPENDIX C

SUMMARY OF HYDRAULIC DATA

Table C.1. Summary of hydraulic data for the outdoor flume (12 ft).[a]

Run[b] No.	D_{50} (in.)	Total Discharge Q_T (cfs)	Surface Discharge Q_s (cfs)	Slope S	Depth D=R (ft)	Velocity V (fps)	Area of Flow A (ft^2)	Froude Number F	Manning's n	Shields' Coefficient C_c	Reynold's Number Re	Darcy-Weisbach Friction Factor f
6	4.10	7.54	3.24	0.20	0.10	2.75	1.18	1.54	0.052	0.035	19283	0.672
6	4.10	10.29	5.99	0.20	0.15	3.27	1.83	1.48	0.058	0.054	24014	0.733
6	4.10	13.00	8.70	0.20	0.12	6.08	1.43	3.11	0.026	0.042	21228	0.166
6	4.10	13.00	8.70	0.20	0.13	5.51	1.58	2.67	0.031	0.047	22313	0.224
6	4.10	13.00	8.70	0.20	0.17	4.18	2.08	1.77	0.049	0.061	25602	0.510
6	4.10	16.10	11.80	0.20	0.17	5.96	1.98	2.59	0.034	0.059	24979	0.239
6	4.10	16.10	11.80	0.20	0.19	5.18	2.28	2.09	0.042	0.067	26804	0.365
6	4.10	16.10	11.80	0.20	0.21	4.66	2.53	1.79	0.050	0.075	28236	0.499
6	4.10	17.50	13.20	0.20	0.17	6.35	2.08	2.69	0.033	0.061	25602	0.222
6	4.10	17.50	13.20	0.20	0.21	5.22	2.53	2.00	0.045	0.075	28236	0.399
6	4.10	17.50	13.20	0.20	0.21	5.22	2.53	2.00	0.045	0.075	28236	0.399
7	4.10	14.10	9.80	0.20	0.23	3.63	2.70	1.35	0.068	0.080	29169	0.880
7	4.10	14.10	9.80	0.20	0.20	4.17	2.35	1.66	0.054	0.069	27213	0.580
7	4.10	16.75	12.45	0.20	0.25	4.15	3.00	1.46	0.064	0.089	30747	0.748
7	4.10	16.75	12.45	0.20	0.17	5.93	2.10	2.50	0.035	0.062	25724	0.257
7	4.10	18.77	14.47	0.20	0.17	7.24	2.00	3.12	0.028	0.059	25104	0.164
7	4.10	18.77	14.47	0.20	0.25	4.82	3.00	1.70	0.055	0.089	30747	0.554
7	4.10	18.77	14.47	0.20	0.18	6.58	2.20	2.71	0.033	0.065	26330	0.218
7	4.10	20.66	16.36	0.20	0.18	7.61	2.15	3.17	0.028	0.064	26029	0.159
7	4.10	20.66	16.36	0.20	0.18	7.79	2.10	3.28	0.027	0.062	25724	0.149
7	4.10	20.66	16.36	0.20	0.28	4.88	3.35	1.63	0.058	0.099	32491	0.603
7	4.10	20.66	16.36	0.20	0.22	6.06	2.70	2.25	0.041	0.080	29169	0.316
7	4.10	20.66	16.36	0.20	0.29	4.67	3.50	1.53	0.063	0.103	33210	0.688
7	4.10	21.78	17.48	0.20	0.18	8.13	2.15	3.38	0.026	0.064	26029	0.140
7	4.10	21.78	17.48	0.20	0.19	7.77	2.25	3.16	0.028	0.067	26627	0.160
7	4.10	21.78	17.38	0.20	0.28	5.22	3.35	1.74	0.054	0.099	32491	0.528

Table C.1. Continued.

Run[b] No.	D_{50} (in.)	Total Discharge Q_T (cfs)	Surface Discharge Q_s (cfs)	Slope S	Depth D=R (ft)	Velocity V (fps)	Area of Flow A (ft^2)	Froude Number F	Manning's n	Shields' Coefficient C_c	Reynold's Number Re	Darcy-Weisbach Friction Factor f
8	5.10	8.75	2.92	0.20	0.07	3.70	0.79	2.54	0.029	0.019	19626	0.248
8	5.10	8.75	2.92	0.20	0.12	2.06	1.42	1.05	0.078	0.034	26313	1.422
8	5.10	11.41	5.58	0.20	0.13	3.62	1.54	1.78	0.047	0.037	27402	0.504
8	5.10	11.41	5.58	0.20	0.18	2.63	2.12	1.10	0.079	0.050	32151	1.314
9	5.10	10.26	4.43	0.20	0.10	3.72	1.19	2.08	0.038	0.028	24088	0.369
9	5.10	10.26	4.43	0.20	0.13	2.91	1.52	1.44	0.058	0.036	27223	0.768
9	5.10	12.54	6.71	0.20	0.14	4.09	1.64	1.95	0.043	0.039	28278	0.421
9	5.10	12.54	6.71	0.20	0.09	6.05	1.11	3.50	0.022	0.026	23264	0.130
9	5.10	12.54	6.71	0.20	0.17	3.24	2.07	1.38	0.064	0.049	31769	0.846
9	5.10	14.53	8.70	0.20	0.17	4.37	1.99	1.89	0.046	0.047	31149	0.447
9	5.10	14.53	8.70	0.20	0.12	6.17	1.41	3.17	0.026	0.034	26220	0.159
9	5.10	14.53	8.70	0.20	0.21	3.52	2.47	1.37	0.066	0.059	34703	0.855
9	5.10	17.56	11.73	0.20	0.22	4.44	2.64	1.67	0.055	0.063	35878	0.574
9	5.10	17.56	11.73	0.20	0.19	5.19	2.26	2.11	0.042	0.054	33195	0.360
9	5.10	17.56	11.73	0.20	0.14	7.07	1.66	3.35	0.025	0.039	28450	0.143
9	5.10	17.56	11.73	0.20	0.24	4.02	2.92	1.44	0.064	0.069	37732	0.777
9	5.10	19.32	13.49	0.20	0.24	4.75	2.84	1.72	0.054	0.067	37212	0.540
9	5.10	19.32	13.49	0.20	0.21	5.48	2.46	2.13	0.042	0.058	34633	0.351
9	5.10	19.32	13.49	0.20	0.17	6.71	2.01	2.89	0.030	0.048	31305	0.192
9	5.10	19.32	13.49	0.20	0.26	4.39	3.07	1.53	0.061	0.073	38689	0.683
9	5.10	19.32	13.49	0.20	0.16	7.10	1.90	3.14	0.027	0.045	30437	0.162
9	5.10	20.61	14.78	0.20	0.25	4.86	3.04	1.70	0.055	0.072	38500	0.552
9	5.10	20.61	14.78	0.20	0.21	5.77	2.56	2.20	0.041	0.061	35330	0.330
9	5.10	20.61	14.78	0.20	0.17	7.17	2.06	3.05	0.029	0.049	31692	0.172
9	5.10	20.61	14.78	0.20	0.26	4.66	3.17	1.60	0.059	0.075	39314	0.626

Table C.1. Continued.

Run[b] No.	D_{50} (in.)	Total Discharge Q_T (cfs)	Surface Discharge Q_s (cfs)	Slope S	Depth D=R (ft)	Velocity V (fps)	Area of Flow A (ft^2)	Froude Number F	Manning's n	Shields' Coefficient C_c	Reynold's Number Re	Darcy-Weisbach Friction Factor f
9	5.10	20.61	14.78	0.20	0.17	7.21	2.05	3.07	0.028	0.049	31615	0.169
9	5.10	20.61	14.78	0.20	0.16	7.74	1.91	3.42	0.025	0.045	30517	0.137
9	5.10	23.93	18.10	0.20	0.29	5.19	3.49	1.69	0.056	0.083	41251	0.557
9	5.10	23.93	18.10	0.20	0.25	5.92	3.06	2.06	0.045	0.073	38626	0.375
9	5.10	23.93	18.10	0.20	0.20	7.51	2.41	2.95	0.030	0.057	34279	0.183
9	5.10	23.93	18.10	0.20	0.30	5.07	3.57	1.64	0.058	0.085	41721	0.596
9	5.10	23.93	18.10	0.20	0.18	8.23	2.20	3.39	0.026	0.052	32752	0.140
9	5.10	23.93	18.10	0.20	0.20	7.67	2.36	3.05	0.029	0.056	33922	0.172
9	5.10	26.19	20.36	0.20	0.29	5.92	3.44	1.95	0.049	0.082	40954	0.422
9	5.10	26.19	20.36	0.20	0.27	6.25	3.26	2.11	0.045	0.077	39869	0.359
9	5.10	26.19	20.36	0.20	0.21	8.11	2.51	3.13	0.029	0.060	34983	0.164
9	5.10	26.19	20.36	0.20	0.31	5.47	3.72	1.73	0.056	0.088	42589	0.533
9	5.10	26.19	20.36	0.20	0.21	7.95	2.56	3.03	0.030	0.061	35330	0.174
11	6.20	7.87	1.65	0.20	0.04	3.30	0.50	2.85	0.024	0.010	18981	0.197
11	6.20	7.87	1.65	0.20	0.05	3.00	0.55	2.47	0.028	0.011	19908	0.262
11	6.20	7.87	1.65	0.20	0.04	3.06	0.54	2.54	0.028	0.011	19726	0.248
11	6.20	13.60	7.38	0.20	0.20	3.01	2.45	1.17	0.076	0.048	42017	1.159
11	6.20	13.60	7.38	0.20	0.18	3.40	2.17	1.41	0.062	0.042	39543	0.805
11	6.20	13.60	7.38	0.20	0.15	4.12	1.79	1.88	0.045	0.035	35915	0.452
11	6.20	13.60	7.38	0.20	0.14	4.39	1.68	2.07	0.041	0.033	34794	0.374
11	6.20	19.47	13.25	0.20	0.30	3.73	3.55	1.21	0.079	0.069	50578	1.094
11	6.20	19.47	13.25	0.20	0.28	3.91	3.39	1.30	0.073	0.066	49425	0.953
11	6.20	19.47	13.25	0.20	0.26	4.25	3.12	1.47	0.064	0.061	47416	0.743
11	6.20	19.47	13.25	0.20	0.24	4.67	2.84	1.69	0.054	0.056	45238	0.560
11	6.20	19.47	13.25	0.20	0.23	4.85	2.73	1.79	0.051	0.053	44353	0.498

Table C.1. Continued.

Run[b] No.	D_{50} (in.)	Total Discharge Q_T (cfs)	Surface Discharge Q_S (cfs)	Slope S	Depth D=R (ft)	Velocity V (fps)	Area of Flow A (ft^2)	Froude Number F	Manning's n	Shields' Coefficient C_c	Reynold's Number Re	Darcy-Weisbach Friction Factor f
12	6.20	12.50	6.28	0.20	0.14	3.81	1.65	1.81	0.047	0.032	34481	0.489
12	6.20	12.50	6.28	0.20	0.17	3.06	2.05	1.31	0.067	0.040	38434	0.938
12	6.20	12.50	6.28	0.20	0.13	4.13	1.52	2.05	0.041	0.030	33095	0.382
12	6.20	12.50	6.28	0.20	0.13	4.08	1.54	2.01	0.041	0.030	33312	0.398
12	6.20	12.50	6.28	0.20	0.12	4.55	1.38	2.36	0.035	0.027	31534	0.286
12	6.20	19.80	13.58	0.20	0.25	4.60	2.95	1.64	0.057	0.058	46106	0.598
12	6.20	19.80	13.58	0.20	0.25	4.45	3.05	1.56	0.060	0.060	46881	0.661
12	6.20	19.80	13.58	0.20	0.24	4.82	2.82	1.75	0.053	0.055	45078	0.522
12	6.20	19.80	13.58	0.20	0.21	5.35	2.54	2.05	0.044	0.050	42782	0.382
12	6.20	19.80	13.58	0.20	0.21	5.26	2.58	2.00	0.045	0.050	43117	0.400
13	6.20	26.50	20.28	0.20	0.31	5.41	3.75	1.70	0.057	0.073	51983	0.550
13	6.20	26.50	20.28	0.20	0.36	4.66	4.35	1.36	0.072	0.085	55987	0.859
13	6.20	26.50	20.28	0.20	0.29	5.93	3.42	1.96	0.049	0.067	49643	0.418
13	6.20	26.50	20.28	0.20	0.35	4.90	4.14	1.47	0.067	0.081	54619	0.741
13	6.20	28.10	21.88	0.20	0.40	4.61	4.75	1.29	0.078	0.093	58505	0.961
13	6.20	28.10	21.88	0.20	0.36	5.03	4.35	1.47	0.067	0.085	55987	0.738
13	6.20	28.10	21.88	0.20	0.37	4.98	4.39	1.45	0.068	0.086	56244	0.579
13	6.20	28.10	21.88	0.20	0.31	5.85	3.74	1.85	0.052	0.073	51913	0.469
13	6.20	31.10	24.88	0.20	0.41	5.03	4.95	1.38	0.073	0.097	59724	0.841
13	6.20	31.10	24.88	0.20	0.37	5.59	4.45	1.62	0.061	0.087	56627	0.611
13	6.20	31.10	24.88	0.20	0.37	5.54	4.49	1.60	0.062	0.088	56881	0.628
13	6.20	31.10	24.88	0.20	0.32	6.40	3.89	1.98	0.049	0.076	52944	0.408
13	6.20	31.10	24.88	0.20	0.30	6.95	3.58	2.24	0.043	0.070	50791	0.318

Table C.1. Continued.

Run[b] No.	D_{50} (in.)	Total Discharge Q_T (cfs)	Surface Discharge Q_s (cfs)	Slope S	Depth D=R (ft)	Velocity V (fps)	Area of Flow A (ft^2)	Froude Number F	Manning's n	Shields' Coefficient C_c	Reynold's Number Re	Darcy-Weisbach Friction Factor f
17	2.20	4.04	2.60	0.20	0.05	4.41	0.59	3.50	0.020	0.033	7316	0.130
17	2.20	4.04	2.60	0.20	0.06	3.42	0.76	2.40	0.031	0.042	8304	0.279
17	2.20	4.04	2.60	0.20	0.06	3.82	0.68	2.83	0.026	0.037	7855	0.200
17	2.20	4.71	3.27	0.20	0.07	3.67	0.89	2.38	0.032	0.049	8986	0.283
17	2.20	4.71	3.27	0.20	0.08	3.24	1.01	1.97	0.039	0.056	9573	0.414
17	2.20	4.71	3.27	0.20	0.07	3.72	0.88	2.42	0.031	0.048	8935	0.274
17	2.20	5.33	3.89	0.20	0.08	4.14	0.94	2.61	0.029	0.052	9235	0.236
17	2.20	5.33	3.89	0.20	0.11	3.09	1.26	1.68	0.048	0.069	10692	0.568
17	2.20	5.33	3.89	0.20	0.09	3.44	1.13	1.98	0.040	0.062	10125	0.409
17	2.20	5.58	4.14	0.20	0.09	3.98	1.04	2.38	0.033	0.057	9714	0.282
17	2.20	5.58	4.14	0.20	0.11	3.29	1.26	1.79	0.045	0.069	10692	0.501
17	2.20	5.58	4.14	0.20	0.10	3.51	1.18	1.97	0.040	0.065	10347	0.412
18	2.20	2.67	1.23	0.20	0.04	2.28	0.54	1.89	0.037	0.030	7000	0.447
18	2.20	2.67	1.23	0.20	0.04	2.67	0.46	2.41	0.028	0.025	6460	0.276
18	2.20	2.67	1.23	0.20	0.04	2.56	0.48	2.26	0.030	0.026	6599	0.314
18	2.20	3.82	2.38	0.20	0.06	3.22	0.74	2.28	0.032	0.041	8194	0.307
18	2.20	3.82	2.38	0.20	0.06	3.13	0.76	2.19	0.034	0.042	8304	0.333
18	2.20	3.82	2.38	0.20	0.07	2.87	0.83	1.92	0.039	0.046	8678	0.433
18	2.20	4.45	3.01	0.20	0.08	3.20	0.94	2.02	0.038	0.052	9235	0.394
18	2.20	4.45	3.01	0.20	0.08	3.20	0.94	2.02	0.038	0.052	9235	0.394
18	2.20	6.05	4.61	0.20	0.11	3.57	1.29	1.92	0.042	0.071	10819	0.434
18	2.20	6.05	4.61	0.20	0.11	3.52	1.31	1.88	0.043	0.072	10902	0.454

Table C.1. Continued.

[a] Definitions

$$F = \frac{Q_s/12}{(gD^3)^{0.5}}$$

$$n = \frac{1.486}{Q_s} D^{2/3} S^{1/2} A$$

$$V = \frac{Q_s}{A} \text{ (in ft/s)}$$

$$f = \frac{8gDS}{V^2}$$

$$A = 12 \times D \text{ (in ft}^2\text{)}$$

$$C_c = \frac{DS}{(G_s-1) D_{50}}$$

$$Re = \frac{D_{50} (gDS)^{0.5}}{\nu}$$

$$\nu = 1.41 \times 10^{-5} \text{ ft}^2\text{/s at } 50^{\circ}\text{F}$$

Note: Data computed by IBM PC; therefore rounding effects may be neglected.

[b] Run numbers 10, 10A, and 15 were not included in the analysis due to instruments freezing during tests.

Table C.2. Summary of hydraulic data for the indoor flume (8 ft).[a]

Run No.	D_{50} (in.)	Total Discharge Q_T (cfs)	Surface Discharge Q_s (cfs)	Slope S	Depth D=R (ft)	Velocity V (fps)	Area of Flow A (ft^2)	Froude Number F	Manning's n	Shields' Coefficient C_c	Reynold's Number Re	Darcy-Weisbach Friction Factor f
1	2.20	24.60	24.27	0.02	0.58	5.28	4.66	1.22	0.026	0.040	11501	0.098
1	2.20	24.60	24.27	0.02	0.57	5.35	4.59	1.25	0.025	0.040	11422	0.095
1	2.20	24.60	24.27	0.02	0.57	5.37	4.58	1.25	0.025	0.040	11402	0.094
2	2.20	48.30	47.97	0.02	0.88	6.88	7.02	1.29	0.025	0.061	14126	0.082
2	2.20	47.20	46.87	0.02	0.74	8.10	5.90	1.64	0.020	0.051	12942	0.053
2	2.20	50.40	50.07	0.02	0.89	7.09	7.11	1.32	0.025	0.062	14214	0.078
3	2.20	43.60	43.27	0.02	0.80	6.84	6.38	1.35	0.024	0.055	13451	0.077
3	2.20	43.60	43.27	0.02	0.75	7.25	6.02	1.47	0.022	0.052	13073	0.065
3	2.20	43.60	43.27	0.02	0.87	6.28	6.94	1.19	0.027	0.060	14046	0.098
4	2.20	46.90	46.57	0.02	0.84	6.96	6.74	1.34	0.024	0.059	13834	0.078
4	2.20	46.90	46.57	0.02	0.75	7.79	6.02	1.58	0.020	0.052	13082	0.057
4	2.20	46.90	46.57	0.02	0.97	6.06	7.74	1.09	0.030	0.067	14825	0.115
5	2.20	52.70	52.37	0.02	0.84	7.81	6.74	1.50	0.022	0.059	13842	0.062
5	2.20	52.70	52.37	0.02	1.01	6.53	8.06	1.15	0.029	0.070	15136	0.102
5	2.20	52.70	52.37	0.02	0.94	7.00	7.53	1.27	0.026	0.065	14624	0.084
6	2.20	55.10	54.77	0.02	0.94	7.33	7.52	1.33	0.025	0.065	14616	0.077
6	2.20	55.80	55.47	0.02	1.01	6.90	8.09	1.21	0.027	0.070	15158	0.092
6	2.20	58.80	58.47	0.02	1.05	6.97	8.43	1.20	0.027	0.073	15477	0.093
7	2.20	34.70	34.37	0.02	0.68	6.41	5.42	1.37	0.023	0.047	12404	0.076
7	2.20	37.50	37.17	0.02	0.80	5.84	6.42	1.15	0.028	0.056	13501	0.106
7	2.20	35.70	35.37	0.02	0.73	6.10	5.86	1.26	0.025	0.051	12898	0.090

Table C.2. Continued.

Run No.	D_{50} (in.)	Total Discharge Q_T (cfs)	Surface Discharge Q_s (cfs)	Slope S	Depth D=R (ft)	Velocity V (fps)	Area of Flow A (ft^2)	Froude Number F	Manning's n	Shields' Coefficient C_c	Reynold's Number Re	Darcy-Weisbach Friction Factor f
8	1.02	10.00	9.89	0.02	0.31	4.02	2.49	1.27	0.023	0.046	3776	0.094
8	1.02	10.00	9.89	0.02	0.33	3.85	2.60	1.19	0.025	0.048	3860	0.107
8	1.02	10.00	9.89	0.02	0.31	4.10	2.44	1.31	0.022	0.045	3739	0.089
9	1.02	15.20	15.09	0.02	0.42	4.52	3.36	1.23	0.025	0.063	4388	0.098
9	1.02	15.20	15.09	0.02	0.45	4.23	3.59	1.11	0.027	0.067	4537	0.119
9	1.02	15.20	15.09	0.02	0.37	5.15	2.95	1.49	0.020	0.055	4113	0.067
10	1.02	18.30	18.19	0.02	0.46	4.95	3.70	1.28	0.024	0.069	4602	0.089
10	1.02	18.30	18.19	0.02	0.50	4.58	3.99	1.14	0.027	0.074	4783	0.111
10	1.02	18.30	18.19	0.02	0.44	5.20	3.52	1.38	0.022	0.066	4491	0.077
11	1.02	8.85	8.74	0.02	0.29	3.88	2.28	1.28	0.023	0.042	3614	0.093
11	1.02	8.85	8.74	0.02	0.32	3.43	2.58	1.06	0.028	0.048	3848	0.135
11	1.02	8.85	8.74	0.02	0.30	3.65	2.42	1.17	0.025	0.045	3727	0.112
12	1.02	8.50	8.39	0.02	0.32	3.32	2.56	1.03	0.028	0.048	3830	0.142
12	1.02	8.50	8.39	0.02	0.31	3.47	2.45	1.11	0.026	0.046	3745	0.125
12	1.02	8.50	8.39	0.02	0.30	3.54	2.40	1.14	0.026	0.045	3708	0.117
13	1.02	12.00	11.89	0.02	0.39	3.83	3.14	1.08	0.028	0.058	4239	0.129
13	1.02	12.00	11.89	0.02	0.37	4.05	2.96	1.18	0.025	0.055	4188	0.109
13	1.02	12.00	11.89	0.02	0.39	3.84	3.13	1.08	0.028	0.058	4234	0.128
14	1.02	15.00	14.89	0.02	0.44	4.31	3.48	1.15	0.026	0.065	4465	0.112
14	1.02	15.00	14.89	0.02	0.44	4.26	3.52	1.13	0.027	0.066	4491	0.115
14	1.02	15.00	14.89	0.02	0.42	4.49	3.34	1.22	0.025	0.062	4377	0.099

Table C.2. Continued.

Run No.	D_{50} (in.)	Total Discharge Q_T (cfs)	Surface Discharge Q_S (cfs)	Slope S	Depth D=R (ft)	Velocity V (fps)	Area of Flow A (ft^2)	Froude Number F	Manning's n	Shields' Coefficient C_c	Reynold's Number Re	Darcy-Weisbach Friction Factor f
15	1.02	17.80	17.69	0.02	0.42	5.25	3.39	1.42	0.021	0.063	4409	0.074
15	1.02	17.80	17.69	0.02	0.41	5.44	3.27	1.50	0.020	0.061	4330	0.066
16	1.02	12.00	11.89	0.02	0.33	4.55	2.64	1.39	0.021	0.049	3889	0.078
16	1.02	12.00	.89	0.02	0.32	4.70	2.55	1.47	0.020	0.048	3824	0.071
16	1.02	12.00	11.89	0.02	0.36	4.21	2.85	1.24	0.024	0.053	4040	0.097
17	1.02	15.00	14.89	0.02	0.40	4.71	3.18	1.32	0.023	0.059	4271	0.086
17	1.02	15.00	14.89	0.02	0.39	4.81	3.12	1.36	0.022	0.058	4228	0.081
17	1.02	15.00	14.89	0.02	0.40	4.69	3.20	1.31	0.023	0.060	4282	0.087
18	1.02	17.90	17.79	0.02	0.43	5.19	3.45	1.39	0.022	0.064	4445	0.076
18	1.02	17.90	17.79	0.02	0.42	5.34	3.35	1.45	0.021	0.062	4383	0.070
19	1.02	10.00	9.89	0.01	0.41	3.04	3.29	0.84	0.025	0.030	3032	0.104
19	1.02	10.00	9.89	0.01	0.40	3.16	3.17	0.88	0.024	0.029	2976	0.093
20	1.02	12.00	11.89	0.01	0.43	3.48	3.45	0.93	0.023	0.031	3104	0.083
20	1.02	12.00	11.89	0.01	0.50	2.98	4.02	0.74	0.029	0.037	3354	0.129
21	1.02	31.70	31.59	0.01	0.77	5.17	6.13	1.04	0.021	0.056	4139	0.062
21	1.02	31.70	31.59	0.01	0.84	4.71	6.74	0.90	0.025	0.061	4339	0.081
21	1.02	31.70	31.59	0.01	0.79	5.01	6.33	0.99	0.022	0.058	4206	0.068
22	1.02	34.50	34.39	0.01	0.80	5.37	6.42	1.06	0.021	0.058	4237	0.060
22	1.02	34.50	34.39	0.01	0.93	4.66	7.41	0.85	0.026	0.067	4550	0.089
22	1.02	34.50	34.39	0.01	0.84	5.13	6.73	0.99	0.023	0.061	4337	0.068

Table C.2. Continued.

Run No.	D_{50} (in.)	Total Discharge Q_T (cfs)	Surface Discharge Q_s (cfs)	Slope S	Depth D=R (ft)	Velocity V (fps)	Area of Flow A (ft^2)	Froude Number F	Manning's n	Shields' Coefficient C_c	Reynold's Number Re	Darcy-Weisbach Friction Factor f
23	1.02	40.00	38.89	0.01	0.95	5.26	7.61	0.95	0.024	0.069	4611	0.072
23	1.02	40.00	38.89	0.01	0.93	5.38	7.43	0.98	0.023	0.068	4558	0.067
23	1.02	40.00	38.89	0.01	0.93	5.36	7.46	0.98	0.023	0.068	4568	0.068
24	1.02	43.00	42.89	0.01	1.06	5.10	8.44	0.87	0.026	0.077	4857	0.083
24	1.02	43.00	42.89	0.01	0.99	5.42	7.93	0.96	0.023	0.072	4707	0.070
24	1.02	43.00	42.89	0.01	0.94	5.72	7.52	1.04	0.022	0.068	4585	0.060
26	1.02	2.70	2.49	0.10	0.08	4.07	0.66	2.49	0.022	0.059	4394	0.127
27	1.02	2.48	2.27	0.10	0.11	2.84	0.87	1.52	0.037	0.078	5039	0.339
28	1.02	3.35	3.14	0.10	0.14	2.93	1.14	1.37	0.043	0.102	5768	0.415
29	2.20	9.00	8.44	0.10	0.21	5.49	1.64	2.14	0.029	0.068	14895	0.167
29	2.20	9.00	8.44	0.10	0.26	4.38	2.06	1.52	0.042	0.085	16678	0.325
29	2.20	9.00	8.44	0.10	0.23	4.91	1.83	1.81	0.034	0.076	15743	0.231
30	2.20	10.00	9.44	0.10	0.20	6.35	1.58	2.52	0.024	0.065	14602	0.120
30	2.20	10.00	9.44	0.10	0.27	4.68	2.14	1.60	0.040	0.088	16999	0.294
30	2.20	10.00	9.44	0.10	0.27	4.68	2.14	1.60	0.040	0.088	16999	0.294
31	2.20	10.00	9.44	0.10	0.23	5.46	1.83	2.01	0.031	0.076	15473	0.187
31	2.20	10.00	9.44	0.10	0.29	4.34	2.30	1.43	0.045	0.095	17655	0.367
31	2.20	10.00	9.44	0.10	0.26	4.83	2.07	1.67	0.038	0.086	16742	0.269
32	2.20	14.50	13.94	0.08	0.37	4.91	2.95	1.43	0.042	0.098	17874	0.289
32	2.20	14.50	13.94	0.08	0.34	5.39	2.69	1.64	0.036	0.089	17056	0.220
32	2.20	14.50	13.94	0.08	0.31	5.87	2.47	1.86	0.031	0.082	16357	0.172

Table C.2. Continued.

[a] Definitions

$$F = \frac{Q_T/8}{(gD^3)^{0.5}}$$

$$n = \frac{1.486}{Q_T} R^{2/3} S^{1/2} A$$

$$V = \frac{Q_T}{A} \text{ (in ft/s)}$$

$$f = \frac{8gRS}{V^2}$$

$$A = 8 \times D \text{ (in ft}^2\text{)}$$

$$C_c = \frac{DS}{(G_S - 1) D_{50}}$$

$$R_e = \frac{D_{50} (gDS)^{0.5}}{\nu}$$

$$\nu = 1.00 \times 10^{-5} \text{ ft}^2\text{/s at } 72^\circ\text{F}$$

Note: Data computed by IBM PC; therefore rounding effects may be neglected.

NRC FORM 335 (2-84) NRCM 1102, 3201, 3202

U.S. NUCLEAR REGULATORY COMMISSION

BIBLIOGRAPHIC DATA SHEET

SEE INSTRUCTIONS ON THE REVERSE

1. REPORT NUMBER (Assigned by TIDC, add Vol. No., if any)
NUREG/CR-4651
ORNL/TM-10100

2. TITLE AND SUBTITLE
Development of Riprap Design Criteria by Riprap Testing in Flumes: Phase I

3. LEAVE BLANK

4. DATE REPORT COMPLETED
MONTH: October YEAR: 1986

5. AUTHOR(S)
S. R. Abt, M.S. Khattak, J.D. Nelson, J.F. Ruff, A. Shaikh, R.J. Wittler/CSU
D.W. Lee, N.E. Hinkley/ORNL

5. DATE REPORT ISSUED
MONTH: May YEAR: 1987

7. PERFORMING ORGANIZATION NAME AND MAILING ADDRESS (Include Zip Code)
Colorado State University
Fort Collins, CO 80523

Under Contract to:
Oak Ridge National Lab.
Oak Ridge, TN 37831

8. PROJECT/TASK/WORK UNIT NUMBER

9. FIN OR GRANT NUMBER
A-9350

10. SPONSORING ORGANIZATION NAME AND MAILING ADDRESS (Include Zip Code)
Uranium Recovery Field Off.
Region IV - Box 25325
U.S. Nuclear Reg. Comm.
Denver, CO 80402

Div. of Waste Management
Office of Nuclear Material Safety and Safeguards
U.S. Nuclear Reg. Comm.
Washington, DC 20555

11a. TYPE OF REPORT
Technical

b. PERIOD COVERED (Inclusive dates)

12. SUPPLEMENTARY NOTES

13. ABSTRACT (200 words or less)

Flume studies were conducted in which riprap embankments were subjected to overtopping flows. Embankment slopes of 1, 2, 8, 10 and 20% were protected with riprap layers with median stone sizes of 1, 2, 4, 5 and/or 6 inches. Riprap design criteria for overtopping flows were developed in terms of unit discharge at failure, interstitial velocities and discharges through the riprap layer, resistance to flow over the riprap surface, potential impacts of the filter blanket on the riprap layer stability, and the effects of flow concentrations on the riprap stability. The resulting riprap design criteria were compared to the Stephenson, the U.S. Army Corps of Engineers, the U.S. Bureau of Reclamation, and the Safety Factors methods for riprap stone design; the Leps relation for interstitial velocities through riprap; and the Anderson et al. and Corps of Engineers relationships for estimating Manning's n values for resistance to flow.

14. DOCUMENT ANALYSIS - a. KEYWORDS/DESCRIPTORS
Riprap Design Criteria, Riprap Stability
Riprap Testing
Riprap
Riprap Embankments

b. IDENTIFIERS/OPEN-ENDED TERMS

15. AVAILABILITY STATEMENT
Unlimited

16. SECURITY CLASSIFICATION
(This page) Unclassified
(This report) Unclassified

17. NUMBER OF PAGES

18. PRICE

UNITED STATES
NUCLEAR REGULATORY COMMISSION
WASHINGTON, D.C. 20555

120555078877 1 1AN
US NRC-OARM-ADM
DIV OF PUB SVCS
POLICY & PUB MGT BR-PDR NUREG
W-501
WASHINGTON DC 20555